Received: 26 November 2019 | Revised: 18 September 2020 | Accepted: 23 October 2020

DOI: 10.1096/fj.201902981R

RESEARCH ARTICLE

THE FASEB JOURNAL

Staphylococcus aureus Panton-Valentine Leukocidin triggers an alternative NETosis process targeting mitochondria

Viola Mazzoleni[1] | **Gaëlle Zimmermann-Meisse**[1] | **Anna Smirnova**[2] | **Ivan Tarassov**[2] | **Gilles Prévost**[1]

[1]University of Strasbourg, CHRU Strasbourg, ITI InnoVec, Fédération de Médecine Translationnelle de Strasbourg, UR7290, Institut de Bactériologie, Strasbourg, France

[2]UMR 7156 GMGM Strasbourg University/ CNRS, Strasbourg, France

Correspondence
Gilles Prévost, University of Strasbourg, CHRU Strasbourg, ITI InnoVec, Fédération de Médecine Translationnelle de Strasbourg, UR7290, Institut de Bactériologie, 3 rue Koeberlé, 67000 Strasbourg, France.
Email: prevost@unistra.fr

Funding information
Ministère de l'Enseignement supérieur, de la Recherche et de l'Innovation (MESRI), Grant/Award Number: UR7290,UMR7156; Labex Mitocros, Universite de Strasbourg, Grant/Award Number: UMR7156

Abstract

Panton-Valentine Leukocidin (PVL) is a bicomponent leukotoxin produced by 3%-10% of clinical *Staphylococcus aureus (SA)* strains involved in the severity of hospital and community-acquired infections. Although PVL was long known as a pore-forming toxin, recent studies have challenged the formation of a pore at the plasma membrane, while its endocytosis and the exact mode of action remain to be defined. In vitro immunolabeling of human neutrophils shows that Neutrophil Extracellular Traps (NETosis) is triggered by the action of purified PVL, but not by Gamma hemolysin CB (HlgCB), a structurally similar *SA* leukotoxin. PVL causes the ejection of chromatin fibers (NETs) decorated with antibacterial peptides independently of the NADPH oxidase oxidative burst. Leukotoxin partially colocalizes with mitochondria and enhances the production of reactive oxygen species from these organelles, while showing an increased autophagy, which results unnecessary for NETs ejection. PVL NETosis is elicited through Ca^{2+}-activated SK channels and Myeloperoxidase activity but is abolished by Allopurinol pretreatment of neutrophils. Moreover, massive citrullination of the histone H3 is performed by peptidyl arginine deiminases. Inhibition of this latter enzymes fails to abolish NET extrusion. Unexpectedly, PVL NETosis does not seem to involve Src kinases, which is the main kinase family activated downstream the binding of PVL F subunit to CD45 receptor, while the specific kinase pathway differs from the NADPH oxidase-dependent NETosis. PVL alone causes a different and specific form of NETosis that may rather represent a bacterial strategy conceived to disarm and disrupt the immune response, eventually allowing *SA* to spread.

Abbreviations: C5aR, C5a complement-derived peptide receptor; citH3, citrullinated histone H3; CytC, cytochrome c; DHR123, dihydrorhodamine 123; DNP, 2,4-dinitrophenol; DPI, diphenyleneiodonium; LC3A and LC3B, light chain of microtubule-associated protein 1a and 1b; LukF-PV, F subunit of PVL; LukS-PV, S subunit of PVL; HlgCB, gamma-hemolysin CB; HOCl, hydrogen peroxide into hypochlorous acid; hPMNs, human neutrophils; MPO, Myeloperoxidase; MRSA, Methicillin-resistant *Staphylococcus aureus*; mtROS, mitochondrial reactive oxygen species; NE, neutrophil elastase; NETosis, neutrophil extracellular traps; NOX, NADPH oxidase; PAD4, peptidyl arginine deiminase 4; PCC, Pearson correlation coefficient; PFA, paraformaldehyde; PKC, protein kinase c; PP1, 4-amino-5-(4-methylphenyl)-7-(t-butyl)pyrazolo[3,4-d]-pyrimidine; PP2, 4-amino-5-(4-chlorophenyl)-7-(t-butyl)pyrazolo[3,4-d] pyrimidine; PVL, Panton-Valentine Leukocidin; ROS, NADPH oxidase-derived reactive oxygen species; SA, *Staphylococcus aureus*; SK, small conductance calcium-dependent potassium channel; XO, xanthine oxidase.

Gaëlle Zimmermann-Meisse and Anna Smirnova are participated equally to this article.

KEYWORDS
colocalization, Leukocidin, mitochondria, NETosis, ROS, SK channels

1 | INTRODUCTION

One-third of the human beings are possible carriers of *Staphylococcus aureus (SA)*, a worldwide spread bacterium responsible for multiple infections.[1] Despite being a commensal bacterium for healthy hosts, this pathogen mainly takes advantage of weakened immunity, thus, representing one of the most common causes of both community and hospital-acquired infections. The pathogenicity of *SA* is due to its ability to easily adapt to human immunity through the production of diverse virulence factors that can strategically counteract various steps of the innate immune response. Thus, this allows the delay of the adaptive immune response and promotes the bacterial spreading to any deep tissues and organs.[2-4] *SA* virulence factors mainly target leukocytes, as in the case of a group of bipartite leukotoxins known as "pore-forming toxins" (PFT).[2] Here, we focused on two of the leukotoxins group: the Panton-Valentine Leukocidin (PVL), which is produced via an integrated bacteriophage and is present in 3%-10% of clinical *SA* strains,[5-7] representing a factor that influences the severity of infection, and the Gamma-hemolysin CB (HlgCB) expressed from the core genome of 99% of *SA* strains, which is mainly related to hemolytic activity.[8-11] Those leukotoxins share several structural characteristics. In fact, PVL and the HlgCB are both composed by two subunits: a slow-eluted compound, the S subunits (31-32 kDa), and a fast-eluted one, the F subunits (34-35 kDa), as the F subunit is eluted before the S subunit during the cation-exchange chromatography.[12] PVL and HlgCB S subunits are called LukS-PV and HlgC, respectively, while the F subunits are LukF-PV and HlgB, respectively. The sequential, but synergistic interaction of S and F subunits at the plasma membrane is required to activate target cells via the phosphorylation of the C5a complement-derived peptide receptor (C5aR).[13,14] More specifically, S subunits of both leukotoxins first interact with the C5aR expressed at the plasma membrane of human neutrophils, macrophages, monocytes, and ganglion neurons,[13,15-17] while the LukF-PV-specific receptor was recently reported to be the CD45.[18]

Albeit PVL and HlgCB were long considered as two analogous pore-forming toxins,[19] it has been previously demonstrated that in a more physiological milieu containing 1 mM of extracellular calcium, hPMNs remain intact for several hours in contact with the two toxins.[15,20,21] In fact, rapid and important mobilization of intracellular calcium stocks takes place into hPMNs, followed by late membrane permeabilization only if in contact with PVL within 3 or 6 hours, depending on toxin concentration. At this longer time-point, about 30% of hPMNs exposed to PVL are positive to early apoptosis, while a greater percentage of cells were propidium iodide positive. Therefore, we focused on the Neutrophil extracellular trap process or NETosis. NETs are DNA/chromatin fiber-like extracellular structures that can be induced by several stimuli, including microorganisms,[22] as an immune defense strategy to mechanically block and enzymatically neutralize pathogens.[23] This programed cell death was previously linked to *SA* secreting PVL strains (*SA* PVL^+) by Pilsczek et al,[24] suggesting that *SA* culture media supernatant containing PVL induces NETosis within minutes without cell lysis. Also, more recently Bhattacharya et al[25] stated that PVL cooperates with HlgAB to produce a biofilm-mediated NET formation. These authors demonstrated that *SA* spent media devoid of PVL is sufficient to undergo NETosis, implying that PVL alone cannot induce NETosis. However, the effect of purified PVL was not directly tested so far, while the assessment of this leukotoxin expression in the biofilm spent media used by these authors only showed the presence of PVL F subunit, but not the S subunit.[25] Therefore, a precise study on PVL direct contribution and intracellular signaling in human neutrophils is still lacking. The abundant literature available on NETosis shows how this is a complicated and a stimulus-dependent process, highlighting the presence of several distinct forms of this same phenomenon, which differentially depend on the enzyme NADPH oxidase (NOX) for the production of ROS. In fact, the NOX-dependent NETosis is induced by Lipopolysaccharide (LPS) or PMA, among others,[26-30] while the NOX-independent NETosis is obtained with stimuli such as the uric acid or the calcimycin, a calcium ionophore produced during *Streptomyces chartreusis* fermentation.[24,31-33] This second form of NETosis leads to an intracellular calcium increase and a subsequent decrease of intracellular potassium concentration.[34] The increase in intracellular calcium leads to the activation of the peptidyl arginine deiminase 4 (PAD4).[31,33,35] Moreover, other sources of ROS, aside from NOX, exist in human neutrophils. Those alternative ROS sources can sustain NETosis, such as MPO, converting hydrogen peroxide into hypochlorous acid (HOCl), mitochondria, producing superoxide through mitochondrial OXPHOS chain activity, and the action of the cytosolic enzyme xanthine oxidase (XO).[35] Additionally, xanthine oxidase is linked to the increase of mitochondrial ROS production,[36] creating positive feedback on this organelle.

Also, Douda et al[37] reported that SK3, a small conductance calcium-dependent potassium channel predominantly expressed in human neutrophils, is involved in NOX-independent NETosis.

Additionally, recent studies have highlighted the role of H3 citrullination (citH3) operated by PAD4 in neutrophils, which is solely found in the NOX-independent NETosis.[38]

Our study aimed to analyze PVL and NETosis in the absence of other *Staphylococcus aureus* elements, to discriminate them from the impact of the HlgCB. Then, we compared the characteristics of antibacterial NETosis to the hallmarks of a likely ineffective or even detrimental form of the process. In the present study, we found another difference between two comparable leukotoxins: the sole PVL, but not HlgCB, causes a significant NETosis in human neutrophils, and in a NOX-independent manner, while involving mitochondria, mitochondrial ROS (mtROS) and MPO. Additionally, this process is abolished by Allopurinol pretreatment of hPMNs, suggesting, but not confirming the involvement of XO. We also found that a subsequently increased autophagy takes place independently of NETosis, while neither Akt and ERK1/2 nor CD45 downstream-linked Src kinases are activated. The PVL NETosis-induced chromatin fibers are not only decorated with NE, MPO, but also citH3, collectively showing several discrepancies in comparison with the PMA-induced NETosis.

These results provide a more comprehensive view of the PVL mechanism and may suggest several therapeutic targets to tackle *SA* PVL^+ infections.

2 | MATERIALS AND METHODS

2.1 | Ethics statement

Buffy coats from healthy adult volunteers, mostly aged of less than 30 years and both sexes were purchased from the "Établissement Français du Sang" (Strasbourg, France). Written consents were collected by the Établissement Français du Sang, which keeps confidential donor information.

2.2 | Isolation of human polymorphonuclear cells (hPMNs)

Human PMNs are prepared from about 50 mL of buffy coats from healthy donors. The cells were isolated within 24 hours after blood donation, as previously described.[14,39] Briefly, human neutrophils were separated from other blood components by density gradient centrifugation with Lymphocytes separation medium (CMSMSL0101, Eurobio Scientific, Les Ulis, France). Erythrocytes are initially removed by the adding of 6% (w/vol) dextran for sedimentation, while the remaining amount is removed with hypotonic lysis with 18 mL of ddH_2O, followed by the addition of 2 mL of NaCl 9%, to perform an osmotic shock for 45 seconds. Finally, hPMNs are filtered to obtain an homogeneous preparation of cells, then, counted and resuspended in an RPMI culture media supplemented with either 10% of fetal bovine serum (FBS) (v/v) (P30-3306, PAN-Biotech, Aidenbach, Germany) or 0.5% of bovine serum albumin (BSA) (wt/v) (04-100-810-C, Euromedex, Souffelweyersheim, France). This method allows obtaining a purity of isolated neutrophils greater than 98%, as counted with a May-Grunwald Giemsa staining.[39] Purified neutrophils were used within 30 minutes for all experiments.

2.3 | Human neutrophils culture media conditions

Human neutrophils (hPMNs) used for all experiments are cultured in Roswell Park Memorial Institute medium 1640 (RPMI, Biowest, Nuaillé, France) supplemented with either 10% of fetal bovine serum (FBS) (v/v) or 0.5% of bovine serum albumin (BSA) (w/v), the latter to obtain a better adherence to Petri dishes during hPMNs cell culture. Cells were then kept at 37°C with 5% of CO_2 in a humidified incubator and tested in contact with Phorbol 12-myristate 13-acetate (P1585, Sigma-Aldrich, St. Louis, Missouri, USA), A23187 (C7222, Sigma-Aldrich, St. Louis, Missouri, USA), or with PVL and HlgCB intoxication for a maximum of 6 hours.

2.4 | Inhibitors

To test PVL NETosis dependence on different enzymes, channels, or organelles, we used a range of several specific inhibitors. More precisely, Diphenyleneiodonium chloride or DPI (D2926, Sigma-Aldrich, St. Louis, Missouri, USA) was used at a 20 μM final concentration applied for 30 minutes to hPMNs before stimuli addition to inhibit NADPH oxidase machinery. Concerning mitochondrial ROS, we pretreated hPMNs with mitochondrial uncouplers, the 2,4-Dinitrophenol (DNP, D198501, Sigma-Aldrich, St. Louis, Missouri, USA) at 750 μM or 10 μM of 2-[[4-(trifluoromethoxy) phenyl]hydrazinylidene] propanedinitrile (FCCP, ab120081, Abcam, Cambridge, UK) for 1 hour to prevent ROS production, preferring this type of inhibitor rather than scavengers that only neutralize already produced ROS.

Allopurinol, a potent xanthine oxidase inhibitor, was purchased from Sigma-Aldrich (A8003, Sigma-Aldrich, St. Louis, Missouri, USA) and used at 2 mM final concentration for 30 minutes before hPMNs stimulation. Myeloperoxidase Inhibitor-I, (sc204107, Santa Cruz Biotechnology, Dallas, Texas, USA), an irreversible and specific inhibitor of the peroxidation activity of MPO, also named ABAH, was used at the final concentration of 100 μM for 30 minutes before the adding of PMA and PVL. Small conductance Ca^{2+}-activated potassium channel (SK)

inhibitor NS8593 hydrochloride and Apamin were purchased from Santa-Cruz Biotechnology (CAS No. 875755-24-1, Santa Cruz Biotechnology, Dallas, Texas, USA) and Sigma-Aldrich (A1289, Sigma-Aldrich, St. Louis, Missouri, USA). NS8593 was used as hPMNs pretreatment at 100 μM, being a reversible SK3-mediated current inhibitor in human and rat SK3, that operates a decrease in calcium sensitivity, while Apamin was used at the final concentration of 200 nM. Cl-amidine (trifluoroacetate salt), an inhibitor of protein arginine deiminases (CAS No. 1043444-18-3, Cayman Chemicals, Ann Arbor, Michigan, USA) was used at 200 μM for 15 minutes before NETosis induction.

The 4-amino-5-(4-methylphenyl)-7-(t-butyl) pyrazolo[3,4-d]- pyrimidine (PP1), a potent but reversible Src kinases Inhibitor, (CAS No. 172889-26-8, Cayman Chemicals, Ann Arbor, Michigan, USA) was used to pretreat hPMNs for 30 minutes before NETosis induction at the final concentration of 5 μM, and 4-amino-5-(4-chlorophenyl)-7-(t-butyl)pyrazolo[3,4-d]pyrimidine (PP2), an irreversible Src kinases inhibitor was purchased from Sigma-Aldrich (P0042, Sigma-Aldrich, St. Louis, Missouri, USA) and used at the final concentration of 10 μM for 30 minutes before NETosis induction.

2.5 | Antibodies and fluorescent dyes

Hoechst dye 32258 (94403, Sigma-Aldrich, St. Louis, Missouri, USA) was employed at the final concentration of 10 μg/mL to stain nuclei and DNA. Dihydrorhodamine 123 (DHR123) fluorescent probe, used for the determination of peroxynitrite and other cytoplasmic ROSs at the final concentration of 2.5 μM, was obtained from Santa Cruz Biotechnology (CAS No. 109244-58-8, Santa Cruz Biotechnology, Dallas, Texas, USA). MitoSOX Red mitochondrial superoxide indicator, purchased from Molecular Probes (M36008, Molecular Probes, Eugene, OR, USA), was used to evaluate mitochondrial superoxide in human neutrophils.

Two main antibodies were used to confirm the presence of NETosis by epifluorescence experiments: the anti-Neutrophil Elastase (ab21595, Abcam, Cambridge, UK, RRID:AB_446409), a polyclonal antibody developed in rabbits and used at the final concentration of 1 μg/mL, and the monoclonal anti-Myeloperoxidase antibody produced in mouse (ab25989, Abcam, Cambridge, UK, RRID:AB_448948), used at the final concentration of 1 μg/mL. The anti-Histone H3 (citrulline R2 + R8 + R17) antibody-ChIP Grade (ab5103, Abcam, Cambridge, UK, RRID:AB_304752), a polyclonal antibody developed in rabbits was used at 1 μg/mL to assess and subsequently quantify the post-translation modification of the histone H3 on the NETs. The secondary antibodies Goat anti-Rabbit IgG (H + L) Cross-Adsorbed Secondary Antibody Alexa Fluor 488 conjugate and Goat anti-Mouse IgM (Heavy chain) Cross-Adsorbed Secondary Antibody, Alexa Fluor 555 conjugate, purchased from Invitrogen (A-11034, RRID:AB_2576217 and A-21426, RRID:AB_2535847, Invitrogen, Waltham, Massachusetts, USA), were used at a concentration of 2 μg/mL in dilution buffer (HBSS-HEPES containing 5% FBS and 1 mg/mL BSA).

For confocal microscopy, we used an antibody raised against the LukS-PV reduced as an antigen-binding $F(ab')^2$ and produced at the Institute of Bacteriology of Strasbourg by Keller D., as previously described.[12,14] A purified Mouse Anti-Cytochrome c, Clone 6H2.B4 purchased from BD Pharmingen (556432, BD Pharmingen, San Diego, CA, USA) was used at 1:100 to stain mitochondria, while DAPI (4′,6-Diamidino-2-phenylindole dihydrochloride) purchased from Sigma-Aldrich (D9542, Sigma-Aldrich, St. Louis, Missouri, USA) was used at 1 μg/mL final concentration to stain DNA and nuclei. The secondary antibodies $F(ab')^2$ Goat anti-Rabbit IgG-$F(ab')^2$ Fragment cross-adsorbed Antibody DyLight 594 Conjugated and the preadsorbed Donkey F(ab')2 Anti-Mouse IgG H&L (Alexa Fluor 488) were used at the final concentration of 2 μg/mL in dilution buffer (HBSS-HEPES containing 5% FBS and 1 mg/mL BSA) and purchased from Bethyl Laboratories, Inc. (A120-212D4, RRID:AB_10698092, Bethyl Laboratories Inc., Montgomery, Texas, USA) and Abcam (ab181289, RRID:AB_2813900, Abcam, Cambridge, UK), respectively.

For immunoblots, we routinely use a polyclonal antibody anti-GAPDH at 1:10 000 (G9545, RRID:AB_796208, Sigma-Aldrich, St. Louis, Missouri, USA) developed in rabbits as a loading control to ensure an equal amount of total proteins for each lane, yet, avoiding stripping and reprobing the Western blot membrane and allowing the evaluation of phosphorylation of tested proteins and total proteins at one glance, in the same image.

To study the phosphorylation of key kinases involved in NETosis, we used primary antibodies at 1:1000 developed in rabbits: an Anti-phospho-Erk1/2 (Thr202/Tyr204, Thr185/Tyr187) monoclonal antibody, recombinant clone AW39R (05-797R, RRID:AB_1587016, Sigma-Aldrich, St. Louis, Missouri, USA), a rabbit monoclonal Anti-phospho Akt (ser 473) (#9271, RRID:AB_329825 Cell Signaling Technologies, Danvers, Massachusetts, USA), and a rabbit polyclonal Anti- Phospho-Src Family (Tyr416) (#2101, RRID:AB_331697, Cell Signaling Technologies, Danvers, Massachusetts, USA).

For autophagy, we used the anti-LC3B (L10382, Invitrogen, Waltham, Massachusetts, USA), a polyclonal antibody developed in rabbits that allows visualizing both LC3A and LC3B bands.

2.6 | Leukotoxin purification

The *SA* HlgCB and PVL toxins were purified as previously described,[40] and leukotoxins mutations and purification also were previously described.[41] Briefly, each subunit of both toxins is purified by affinity chromatography on Glutathione-Sepharose 4B, followed by cation-exchange fast-performance liquid chromatography after removing the GST tag with PreScission Protease (27084301, GE Healthcare, Chicago, Illinois, USA). The homogeneity of preparations is assessed by radial gel immunoprecipitation and by SDS-polyacrylamide gel electrophoresis before storage at −80°C.[41]

2.7 | Immunocytochemical detection of NETosis by epifluorescence microscopy and quantification

Primary antibodies raised against human neutrophil elastase (NE), myeloperoxidase (MPO), and citrullinated histone H3 (citH3) were used to detect NETs in non-permeabilized human neutrophils. Cells (5×10^5 cells/mL in RPMI-0.5% BSA) were maintained for 10 minutes, 1, 3, and 6 hours at 37°C, in a 5% of CO_2 incubator with 1 nM, 0.25 nM, and 0.1 nM of PVL or 50 nM of PMA. The same experiment was initially performed using 1 nM, 0.5 nM, and 0.1 nM of HlgCB to assess the different cellular outcomes of the two toxins. Toxin concentrations are chosen in regards to dissociation constants (Kd) between the toxins and the common target receptor C5aR in human neutrophils.[15] Where indicated, pretreatments with different inhibitors are performed in parallel during 15, 30 minutes, or 1 hour before stimuli addition, depending on the inhibitor. After each incubation period, cells were fixed for 5 minutes with 4% (v/v) paraformaldehyde-HBSS-HEPES and maintained in blocking buffer (10% FBS (v/v), 5 mg/mL BSA in PBS (w/v)) overnight at 4°C after one washing step with Hanks' Balanced Salt Solution (HBSS) supplemented with 10 mM HEPES. Cells were washed twice with HBSS before adding the primary antibodies diluted at 1 µg/mL in the dilution buffer (HBSS-HEPES containing 5% FBS and 1 mg/mL BSA) and maintained 1 hour at RT with gentle agitation. After two HBSS washes, cells were incubated with secondary antibody coupled to Alexa Fluor 488 or Alexa Fluor 555 at a concentration of 2 µg/mL in dilution buffer (HBSS-HEPES containing 5% FBS (v/v) and 1 mg/mL BSA (w/v)) for 1 hour at RT with gentle agitation. Then, cells were washed and incubated for 30 minutes with 10 µg/mL Hoechst 32258 for nuclei and DNA labeling, and then, observed. The observations were made with the Olympus BX60, an epifluorescence upright microscope equipped with a 10 × objective and a filter set which includes a UV filter for visualization of Hoechst fluorescence, a Fluorescein filter, specific for Alexa488 fluorescence, and a Rhodamine filter, for Alexa555 fluorescence. Fluorescent images were analyzed with CellProfiler software version 2.2 for Windows (RRID:SCR_007358, Brod Institute, Harvard, Cambridge, MA, USA),[42] which allows the identification and count of Hoechst-positive cells and NE-, MPO-, or citH3-positive cells. Results are obtained by a sequence of modules forming a pipeline, which are described and can be downloaded at: https://cellprofiler.org/published-pipelines. The percentage of NETing hPMNs was determined by the following formula: secondary antibody-stained cells (ie, NE-positives cells)*100/ Hoechst-stained cells. Thus, we consider the simultaneous presence of DNA and antimicrobial proteins on NETs. This method is based on an adapted version of the formula previously described by Brinkmann and colleagues in 2012.[43] Moreover, two supplementary quantification methods were initially used to confirm Cell Profiler data. Thus, we analyzed Hoechst images with DNA Area and NETosis Analysis (DANA) software, which allows to determine the mean area of cells taking into account swelling of nuclei and decondensation of chromatin,[44] while Squassh by Fiji/ImageJ was used to determine the colocalization between Hoechst and anti-NE antibody fluorescence.[45]

2.8 | Western Blot

Human neutrophils (1×10^7/mL) were incubated, in RPMI-10% FBS (v/v) medium alone or with PMA or PVL at 37°C with 5% of CO_2, for up to 100 minutes. After each incubation time-point, cells were harvested, washed twice with cold PBS, and the pellets were subjected to protein extraction with RIPA buffer supplemented with 0.2% of Triton X-100 (v/v) in the presence of the Protease Inhibitor Cocktail cOmplete (11697498001, Roche, Bâle, Switzerland), $NaVO_3$ (1 mM), leupeptin (25 µM), pepstatin (25 µM), aprotinin (25 µM), NaF (25 mM), levamisole (1 mM), PMSF (1 mM), and phosphatase inhibitors (P5726, Sigma-Aldrich, Saint-Quentin-Fallavier, France). Total protein concentration was determined with a protein assay reagent kit (Thermo Scientific Pierce 660 nm Protein Assay, 22660, Waltham, Massachusetts, USA). The lysates were added to a 4 × loading buffer containing 10% (v/v) of β-mercaptoethanol, 5 mM EDTA, 5 mM EGTA, leupeptin (10 µg/mL), pepstatin (10 µg/mL), aprotinin (10 µg/mL), NaF (10 mM), $NaVO_3$ (5 mM), and levamisole (1 mM) and heated for 5 minutes at 95°C. Protein migration was performed in a sodium dodecyl sulfate 4%-20% gradient polyacrylamide gel electrophoresis (SDS-PAGE) purchased from Bio-Rad and transferred to a 0.22 µm nitrocellulose membrane (GE Healthcare Amersham Protran Supported NC Nitrocellulose Membranes, Chicago, Illinois, USA) for 1 hour at 30 V in a blotting system (Bio-Rad, Hercules, California, USA). Membranes were placed in

blocking buffer (PBS with 5% no fat dry milk) for 3 hour at 4°C with gentle agitation and incubated overnight at 4°C with rabbit primary antibody (1:1000). Immunoblotting with rabbit polyclonal antibody to GAPDH (1:10000) was used as the internal loading control to ensure equivalent amounts of protein in each lane, avoiding the stripping step on nitrocellulose membranes after the revelation of phosphorylated forms of proteins of interest. Detection was achieved using appropriate HRP-linked secondary antibodies (1:50 000), followed by Clarity Max Western ECL Blotting Substrate chemiluminescence kit (#1705062, Bio-Rad, Hercules, California, USA). Immunoreactive bands were visualized with a ChemiDoc Instrument (Bio-Rad, Hercules, California, USA) and quantified with ImageJ (NIH).

2.9 | Flow cytometry for ROS quantification

To measure ROS levels, human neutrophils (1×10^6/mL RPMI without Phenol Red supplemented with 10% (v/v) FBS) were purified and stained with 10 μM of Dihydrorhodamine or 2.5 μM of MitoSOX kept at 37°C for 30 minutes to let the dyes enter the cells. In parallel, the pretreatment with DNP was performed within 1 hour before toxins addition. Then, PMA at 50 nM, PVL at 1 nM, and at 0.25 nM were added, and the acquisition was started. Cells were analyzed with Guava easyCyte 8HT system flow cytometer (EMD, Millipore, Burlington, Massachusetts, USA). The neutrophil population at 1×10^6/mL was analyzed at a medium flow rate of 0.59 μL/s and selected based on Forward Scatter (FSC) and Side Scatter (SSC) parameters. DHR123 or MitoSOX fluorescence was analyzed in the Green (525/30 nm) and Yellow channel (583/26 nm), respectively. The mean Fluorescence intensity (MFI) of both dyes was compared with MFI of unstimulated cells.

2.10 | Immunofluorescence labeling of PVL and mitochondria, confocal microscopy, and image analysis

Freshly isolated hPMNs at 8×10^6 cells/mL in RPMI-10% FBS (v/v) were kept for 5, 10, 15, 20, 30, 40, and 50 minutes at 37°C, in a 5% of CO_2 incubator in the presence of either 1 nM of the PVL or 1 nM of the subunit LukS-PV only. Then, cells were fixed by 4% (v/v) paraformaldehyde-HBSS-HEPES during 10 minutes at room temperature (RT). Next, hPMNs were permeabilized in 0.05% (v/v) Triton X-100 containing HBSS-HEPES for 5 minutes and washed before being blocked for an additional 30 minutes at RT. Another wash was performed prior to the addition of primary antibodies diluted in HBSS-HEPES containing 5% of FBS and 1 mg/mL of BSA. Cells were kept overnight at 4°C and two washes were performed with HBSS-HEPES. Next, secondary antibodies were applied to cells for 1 hour at RT, washed twice, and then, stained for 5 minutes by 1 μg/mL DAPI for labeling nuclei. Cells were mounted on slides using Mowiol media (Mowiol 4.88; cat# 475904; Calbiochem, La Jolla, CA, USA), and stored at 4°C in a light-proof container. The observations were carried out using a Zeiss LSM 780 confocal microscope controlled by the ZEN 2010 with a 63 × oil immersion objective. Ten fields of 1024 × 1024 pixels were acquired for each condition using a 305 nm diode (ultraviolet), a 488 nm argon laser, and a 561 nm diode-pumped solid-state laser. Images were analyzed with the Fiji plug-in MosaicSuite by Squassh (segmentation and quantification of subcellular shapes) tool (RRID:SCR_002285),[45,46] in order to perform segmentation and quantifications of Pearson's correlation coefficient and an overlapping area of LukS-PV fluorescence with CytC fluorescence area. As explained by Rizk and colleagues,[45] this software uses the following intensity-based colocalization equations for a two-channel image:

$$= \frac{\text{Channel1signalcolocalizationinchannel2}}{\text{totalsignalinthecolocalizingregioninchannel1}}$$
$$\text{totalsignalpresentinchannel1altogether}$$

2.11 | Statistical methods

Results are expressed as mean ± standard error of the mean of at least three independent experiments. GraphPad Prism version 7 for Windows software (GraphPad Software, RRID:SCR_002798, La Jolla, CA, USA) was used to calculate the means for each experimental condition, create the graphs, and to obtain the statistical analysis. Student's *t* test and two-way or one-way analysis of variance (ANOVA) followed by a Bonferroni, Dunnett, or Tukey's posttest, were used where appropriate, to detect differences between conditions. A P value $< .05$ was considered significant.

3 | RESULTS

3.1 | PVL, but not HlgCB elicits NE-decorated chromatin fibers spreading in extracellular space

To assess whether a NETosis process is elicited by *SA* leukotoxins, we performed several and separate immunofluorescence assays on non-permeabilized human neutrophils (hPMNs) at definite time-points. Cells were stimulated with either purified PVL or HlgCB at specific and low concentrations. PMA, a NOX-dependent NETosis inducer, was routinely used at 50 nM, mainly as a positive control, while A23187, also known as Calcimycin, was used at the final concentration of 4 μM to initiate a NOX-independent NETosis. Our results

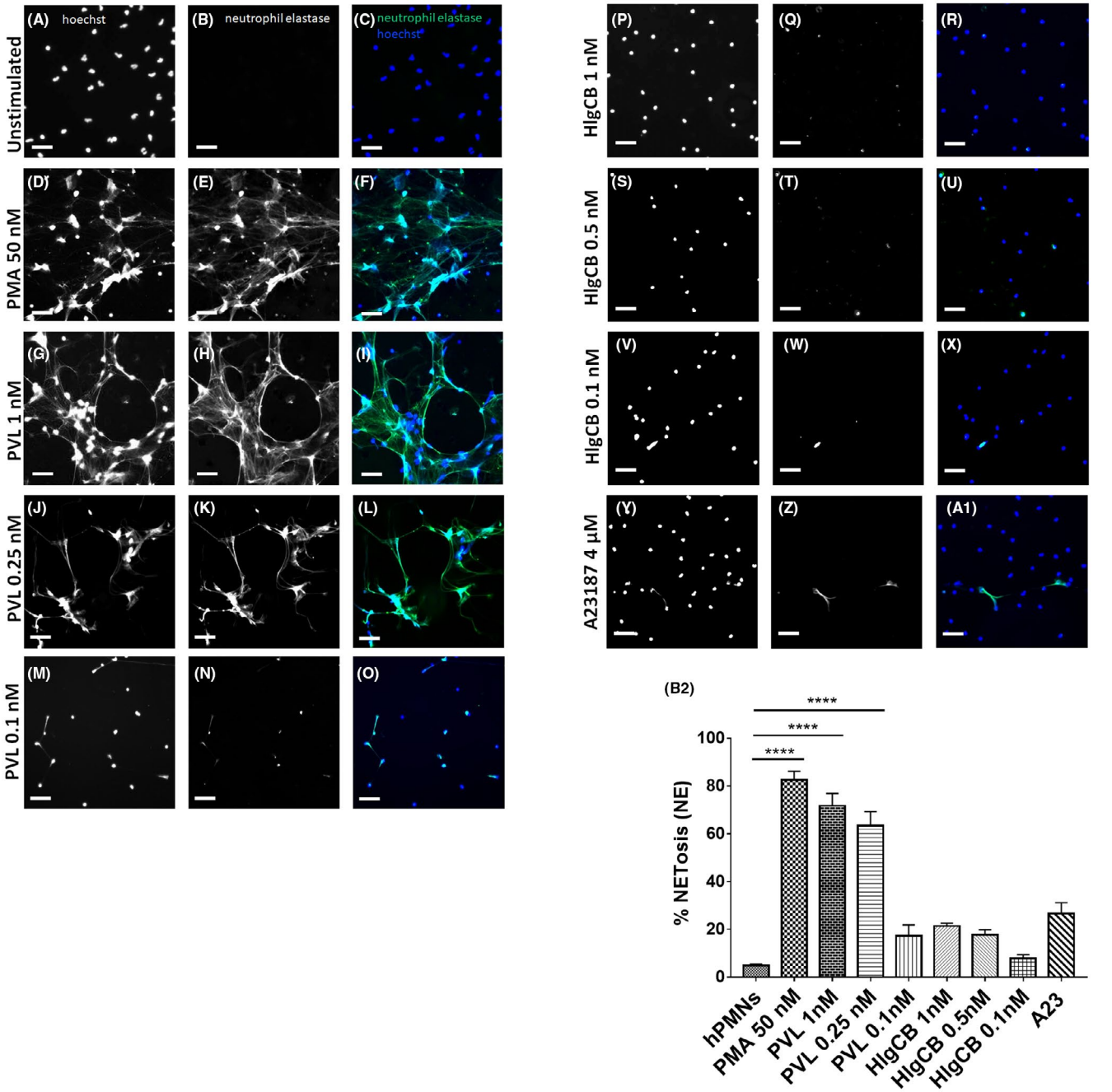

FIGURE 1 PVL, but not HlgCB, elicits NE-decorated chromatin fibers spreading in extracellular space. Freshly isolated human neutrophils (hPMNs) were left unstimulated (A-C) or exposed for 6 hours to PMA at 50 nM (D-F), PVL at 1 nM (G-I), 0.25 nM (J-L), 0.1 nM (M-O), HlgCB at 1 nM (P-R), 0.5 nM (S-U) 0.1 nM (V-X), or A23187 at 4 µM (Y-A1). (Scale bar, 100 µm.) Images are representative of at least three independent experiments. hPMNs were fixed with 4% of PFA and stained with an anti-Neutrophil Elastase (NE) antibody (in green) and Hoechst dye to observe chromatin and nuclei (in blue). (B2) NE-positive cells were quantified using eight random fields of view obtained from three or more different biological replicates. Presented is the mean with SEM. Groups were compared to unstimulated neutrophils using repeated measures one-way ANOVA and Bonferroni posttest, ****$P \leq .0001$, no marks: nonsignificant

show a significant increase of ejected NE associated to extracellular DNA after 6 hours at both 1 nM (Figure 1G–I) and 0.25 nM (Figure 1J–L) of the PVL, concerning about 70% of the total amount of tested neutrophils (Figure 1B2, P value $< .0001$ compared to unstimulated cells). Moreover, the Pearson correlation coefficient was examined. The latter value reaches 0.74 at 6 hours for 1 nM of PVL (Figure S1A). hPMNs exposed to PVL also present a corresponding significant level of MPO associated to extracellular chromatin fibers (Figure S1B), and the mean area of decondensed DNA reaches about 190 µm^2 for 1 nM of PVL, generally confirming that PVL causes a *bona fide* phenomenon of NETosis

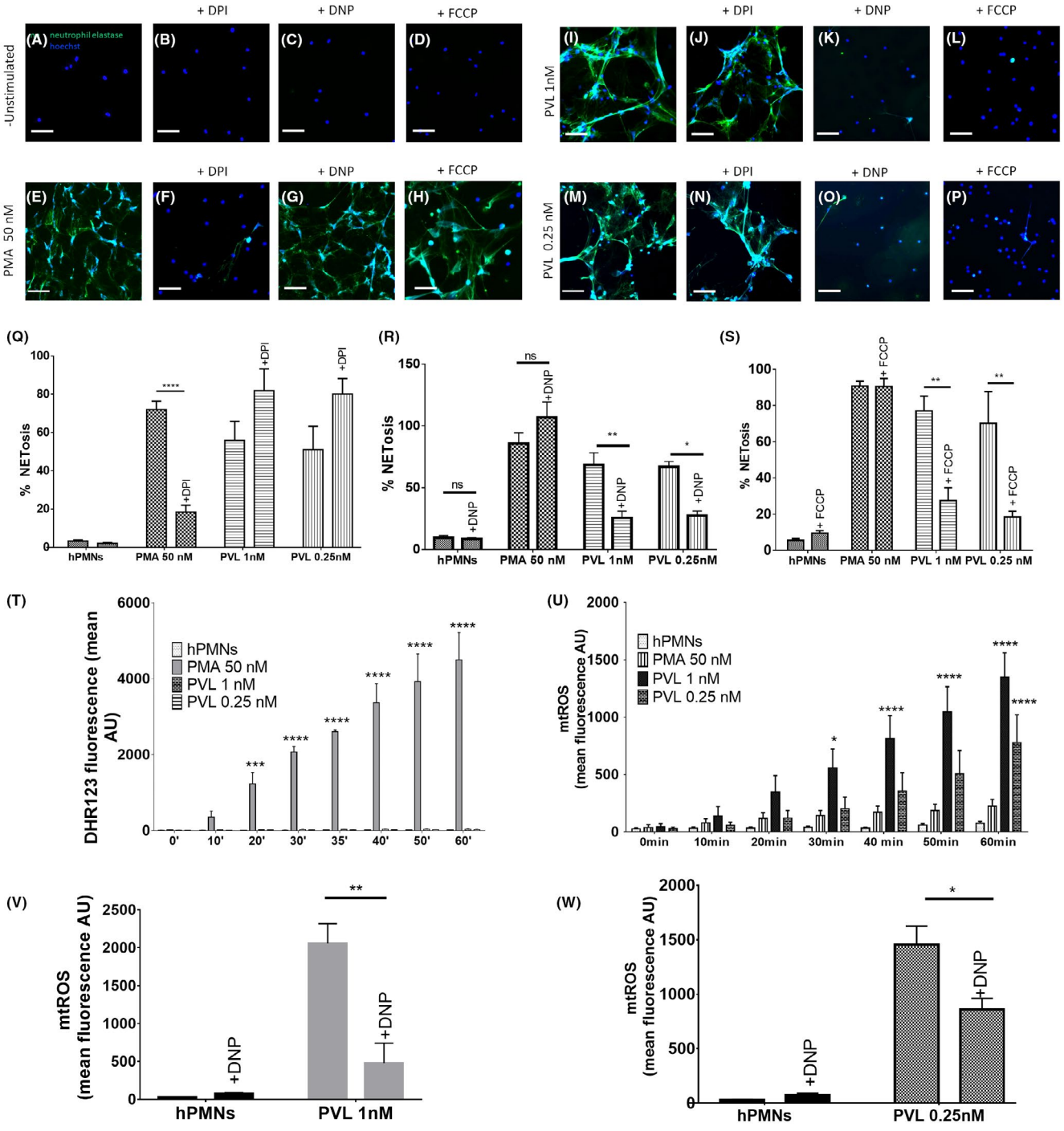

FIGURE 2 PVL-mediated NETosis is independent of NADPH oxidase complex but dependent on mitochondria. (A-P) Immunofluorescence staining Neutrophil Elastase (in green) and DNA with the Hoechst dye (in blue). hPMNs were left unstimulated (A), exposed to 50 nM of PMA (E) or PVL at 1 nM (I) and 0.25 nM (M) during 6 hours. Pretreatments with 20 μM of DPI or 750 μM of DNP and 10 μM of FCCP is performed during 30 and 60 minutes, respectively, before stimulation where indicated (B-D, F-H and I, J-L, and N-P). (Scale bar = 100 μm). (Q-S) NE-positive cells were quantified using eight fields of view obtained from four different biological replicates. Presented is the mean with SEM. Groups were compared using repeated measures two-way ANOVA, $^{****}P \leq .0001$, $^{**}P \leq .01$, $^{*}P < .05$, ns = nonsignificant. (T) Flow cytometry analysis of cytosolic ROS production in hPMNs following DHR123 fluorescence, or with a mitochondrial ROS probe MitoSOX (U) in the presence of 50 nM of PMA, 1 nM and 0.25 nM of PVL or unstimulated after 1 hour. (V and W) Flow cytometry analysis of hPMNs loaded with MitoSOX, after 1 hour with 1 nM (V) and 0.25 nM of PVL (U) in the presence or absence of 750 μM of DNP, preincubated 1 hour prior to stimulation. Presented is the mean with SEM of three different biological replicates. Groups were compared using repeated measures two-way ANOVA, $^{**}P \leq .01$

(Figure S1C). As expected, PMA at 50 nM also causes a significant NETosis at 6 hours (Figure 1D–F), which concerns up to 80% of hPMNs (Figure 1B2). Conversely, 0.1 nM of PVL at 6 hours (Figure 1M–O) as well as HlgCB at 1 nM, 0.5 nM, and 0.1 nM, cause NETosis in only about 20% of hPMNs. Therefore, HlgCB fails to trigger any NETosis within 6 hours (p value > .9999 compared to unstimulated cells) (Figure 1P–X), showing an insignificant number of NE positive hPMNs (Figure 1B2). Surprisingly, A23187 does not cause an appreciable level of NETosis and does elicit the phenomenon in less than 30% of hPMNs (P value > .05 compared to unstimulated cells). Taken together, our results show that purified PVL alone triggers NETosis in vitro, while HlgCB does not.

3.2 | PVL-mediated NETosis is independent of NADPH oxidase complex but dependent on mitochondria

Subsequently, we focused on the involvement of NOX in PMA and PVL-induced NETosis. NOX was inhibited by pretreating hPMNs with 20 μM of Diphenyleneiodonium (DPI), a potent inhibitor of NADPH oxidase, prior to adding the stimuli. NETosis level was quantified at 6 hours, through anti-NE antibody staining. Our results show that DPI significantly inhibits PMA-induced NET formation (Figure 2F), while PVL elicits NETosis in the absence of NOX activity, rather showing an increased amount of NETs after DPI pretreatment (Figure 2J,N). In fact, in the presence of DPI, 1 nM and 0.25 nM of PVL elicit NETosis in about 30% additional hPMNs, compared to the same conditions without DPI pretreatment (Figure 2Q).

Next, we directly investigated the source of the PVL-induced oxidative burst, which is independent of the NADPH oxidase activity. In fact, the classical microbicidal form of the process involves NADPH oxidase as the primary source of reactive oxygen species (ROS), which is necessary for intracellular granules content release.[47] These ROS are usually quantified by flow cytometry with a fluorescent indicator, the dihydrorhodamine 123 (DHR123) at 2.5 μM. DHR123 is a nonfluorescent membrane-permeable ROS indicator that becomes fluorescent in its oxidized form, rhodamine 123, emitting a green fluorescence mainly in the presence of cytosolic reactive oxygen species originated by NOX. The mean fluorescence of DHR123 in hPMNs stimulated with 1 nM and 0.25 nM of PVL shows a nonsignificant generation of cytosolic ROS at any PVL concentrations (Figure 2T). On the contrary, the positive control PMA at 50 nM fosters a very abundant and time-dependent production of ROS from hPMNs (Figure 2T). This confirms that PVL causes NETosis independently of NADPH oxidase ROS.

Human neutrophils possess other ROS sources aside from the NADPH oxidase.[37] We primarily focused on mitochondria, which produces reactive oxygen species, such as superoxide radicals (mtROS). This mitochondrial oxidative burst can be quantified with MitoSOX Red at 2.5 μM, a fluorescent probe, which specifically localizes into this organelle. Flow cytometry experiments showed an opposite situation compared to our DHR123 tests. In fact, after 30 minutes, the mtROS level rapidly increases when hPMNs are in contact with 1 nM of PVL (Figure 2U, P value = .0297) compared with unstimulated cells. At 1 hour, hPMNs produce a significant generation of mtROS in contact with only 0.25 nM of PVL (Figure 2U, P value < .0001) compared to unstimulated cells. Conversely, PMA at 50 nM shows a nonsignificant level of mtROS at each of the examined time-points (Figure 2U, P value = .9525 compared to unstimulated cells).

To further confirm the involvement of mtROS, we tested the effect of the uncoupler of the oxidative phosphorylation 2,4-Dinitrophenol (DNP), which interferes with mitochondrial ROS production.[37] Several flow cytometry assays showed significant inhibition of mtROS production in the presence of 750 μM of DNP for hPMNs exposed to PVL (Figure 2V,W). Therefore, we pretreated hPMNs with DNP, and then, performed immunofluorescence experiments to quantify the PVL NETosis. Our results showed that DNP significantly decreases the PVL NET formation in hPMNs exposed to both 1 nM (Figure 2K) and 0.25 nM of the leukotoxin (Figure 2O), while NETosis resulted decreased in about 40% of total hPMNs (Figure 2R). On the contrary, PMA did not show any NETosis inhibition due to DNP (Figure 2G,R). Additionally, FCCP, another mitochondrial uncoupler was applied to hPMNs prior to stimulation, confirming that the disruption of mtROS generation causes a decrease of PVL NETosis (Figure 2L,P,S). Thus, PVL triggers NET formation via an alternative pathway, involving mitochondria, but not the NADPH oxidase machinery as a source of ROS.

3.3 | PVL NETosis depends on small conductance potassium channels SK and myeloperoxidase (MPO) and is decreased by Allopurinol pretreatment

Based on previous studies,[37] we investigated the contribution of small conductance calcium-activated potassium channels (SK), as this channel is directly involved in the alternative NETosis pathway induced by calcium ionophores. We also focused on an additional ROS source: Myeloperoxidase (MPO).[35] Thereby, we performed pharmacological inhibitions to reduce the SK channel activity by pretreating hPMNs with 100 μM of SK channel inhibitor NS8593 (Figure 3B,F,J,N) or 200 nM of apamin (Figure S3). Then, we

assessed extracellular NE and ADN presence after 6 hours of incubation. Our results confirm the involvement of SK potassium channels in PVL-induced NETosis (Figure 3J,N), unlike with PMA NETosis (Figure 3F). In fact, for both PVL concentrations in the presence of this SK inhibitor, the NETosis rate decreases in about 50% of hPMNs, compared with PVL NETosis in the absence of the same inhibitor. (Figure 3Q). Moreover, we tested the amount of mtROS in the presence of SK inhibitors showing that the disruption of this kind of potassium channels family causes a partial, yet, significant decrease of PVL-induced mitochondrial oxidative burst (Figure 3R).

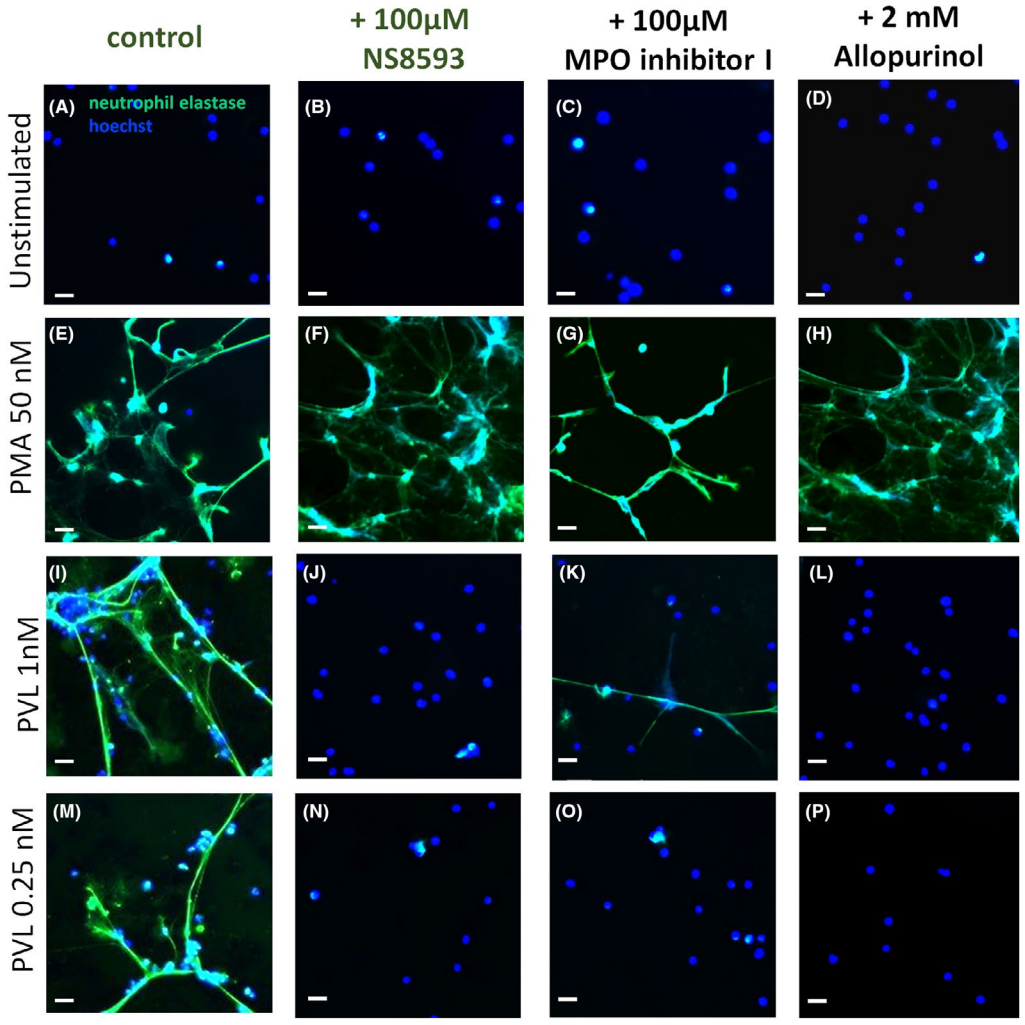

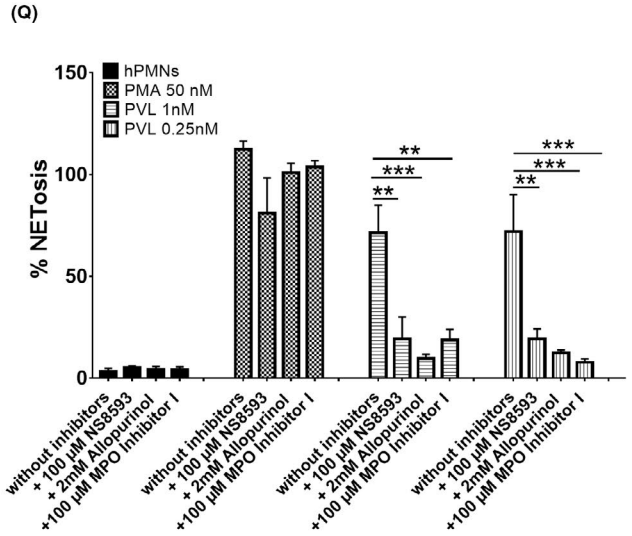

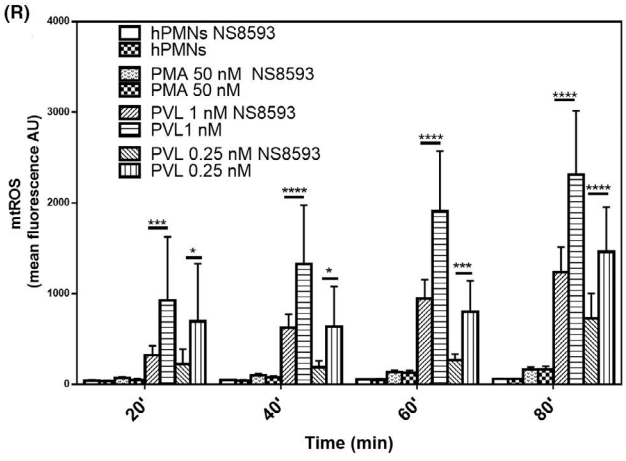

FIGURE 3 PVL NETosis depends on small conductance potassium channels SK and myeloperoxidase (MPO) and is decreased by Allopurinol pretreatment. (A-P) Immunofluorescence staining of hPMNs NE (in green) and DNA (in blue). Cells were left unstimulated (A-D) or exposed to 50 nM of PMA (E-H), PVL at 1 nM (I-L), and PVL 0.25 nM (M-P) after 6 hours in the absence or presence of 100 μM of the SK inhibitor NS8593 (B, F, J, and N), 100 μM of Myeloperoxidase inhibitor I (C, G, K, and O), or 2 mM of Allopurinol (D, H, L, and P) applied during 30 minutes before the incubation. (Q) NE-positive cells were quantified using eight fields of view obtained from three different biological replicates. Presented is the mean with SEM. Groups were compared using repeated measures two-way ANOVA, $^{**}P < .01$. Scale bar = 10 μm. (R) mtROS in the presence or absence of 100 μM of the SK inhibitor NS8593. hPMNs were pretreated with NS8593 for 1 hour prior to stimulation. Cells were left unstimulated or exposed to 50 nM of PMA, 1 nM, or 0.25 nM of PVL. MitoSOX fluorescence was analyzed after 20, 40, 60, and 80 minutes. Data represent mean fluorescence ± SEM from five independent experiments. Groups were compared using repeated measures two-way ANOVA, and Tukey's multiple comparisons test. $^{****}P \leq .0001$, $^{***}P \leq .001$, $^{*}P < .05$

Moreover, we studied the impact of myeloperoxidase (MPO) inhibition, by pretreating hPMNs with MPO inhibitor I (100 μM), followed by immunofluorescence assays. PVL NETosis is dependent on MPO (Figure 3K,O), as the inhibitor significantly decreased NETosis in about 50%-60% of cells in contact with PVL (Figure 3Q), compared to the initial PVL NETosis level. Conversely, PMA showed an opposite result: this NETosis is not inhibited by 100 μM of MPO inhibitor I (Figure 3G,Q).

In parallel, we treated hPMNs with 2 mM of Allopurinol prior to stimulation, as this compound is described to be protective for the mitochondrial membrane integrity while having a strong inhibition activity on the Xanthine Oxidase (XO), another superoxide source present in neutrophils.[35] PVL NETosis is almost completely abolished by Allopurinol treatment (Figure 3L,P), and hPMNs positive to extracellular NE were decreased at about 10% of the totality of cells (Figure 3Q).

Collectively, these results indicate that PVL NETosis is dependent on SK channels and MPO, while Allopurinol seems to inhibit a key step of this process leading to an evident decrease of PVL-induced NETs.

3.4 | PVL, but not PMA, promotes citrullinated histone 3 on NETs, depending on PAD4 activity

A discussed aspect about NETosis process is the presence of a particular posttranslational modification of the histone 3 (H3), named citrullination or deimination (citH3), which transforms the positively charged arginine residues into neutral citrulline. Therefore, immunofluorescence assays allowed the assessment of citH3 in hPMNs, using an anti-citH3 primary antibody. CitH3 was studied after 6 hours hPMNs were exposed to 50 nM of PMA, or 1 nM or 0.25 nM of the PVL. Albeit PMA does not provoke any significant citrullination of the histone H3 (Figure 4D–F), 1 nM and 0.25 nM of PVL favor the citrullination of the histone H3 on NETs after a 6 hours-stimulation (Figure 4G–L). This posttranslational modification concerns about 70% of hPMNs stimulated with 1 nM of PVL and 30% of hPMNs stimulated with 0.25 nM of PVL (Figure 4M).

Then, we wondered whether the mitochondrial uncoupler DNP can also inhibit the citH3. Immunofluorescence imaging and quantification show that DNP decreases the citH3 caused by PVL at 1 nM (Figure 4O) and 0.25 nM (Figure 4P). The corresponding inhibition of citH3 concerns about 40% of tested hPMNs exposed to both PVL concentrations (Figure 4T).

Also, as the occurrence of protein citrullination is caused by a Ca^{2+}-dependent enzyme highly expressed in peripheral blood neutrophils, the peptidylarginine deiminase 4 (PAD4), we evaluated the citH3 level in the presence of 200 μM of Cl-amidine, a pan-PADs inhibitor that inactivates the calcium-binding activity of PAD4 in an irreversible manner.[48] After 6 hours, PVL-induced citH3 is drastically reduced in presence of Cl-amidine for PVL at both 1 nM (Figure 4R) and 0.25 nM (Figure 4S), thus, showing inhibition in 77% and 39% of hPMNs, respectively, compared to citH3 level provoked by PVL in the absence of Cl-amidine (Figure 4U). Nevertheless, in the presence of Cl-amidine, PVL NETs remain evident, as shown by the Hoechst dye staining, and a parallel immunostaining of NE confirms that NETosis process is not prevented by the PAD inhibitor. (Figure 4W,X). Thus, PVL triggers a mitochondrial- and PAD4-dependent presence of citH3 on NETs. However, the PAD4 inhibition does not affect the chromatin and NE liberation, while PMA does not elicit histone H3 citrullination.

3.5 | ERK1/2 and Akt kinases are not phosphorylated by PVL, as well as CD45 downstream kinases are not involved in PVL NETosis

All the abovementioned differences between PMA and PVL made us move forward and question about kinases activated during NETosis. As already highlighted by Douda et al,[37] NOX-dependent and independent NETosis do not exactly share the same signaling pathway. Therefore, we performed different immunoblots to assess the activation of ERK1/2 and Akt, since these two kinases are described as differently involved in PMA-induced and NOX-independent NETosis. As expected, we observed strong phosphorylation of ERK1/2

when human neutrophils were stimulated with 50 nM of PMA for only 15 minutes of incubation (Figure 5A,B). Conversely, PVL fails to significantly activate this kinase (Figure 5A,B). Similarly, Akt is phosphorylated only with 50 nM of PMA after 15 minutes (Figure 5C,D). In fact, PVL at both 1 nM and 0.25 nM does not increase the phosphorylation of this kinase. Indeed, PVL phospho-Akt signal results even lower than hPMNs in the absence of stimulus, which might suggest inhibition of the kinase due to the leukotoxin (Figure 5C,D).

Moreover, as the CD45 receptor is specifically targeted by the LukF-PV subunit of PVL,[18] we studied another kinase family, the Src kinases, being part of the CD45 downstream

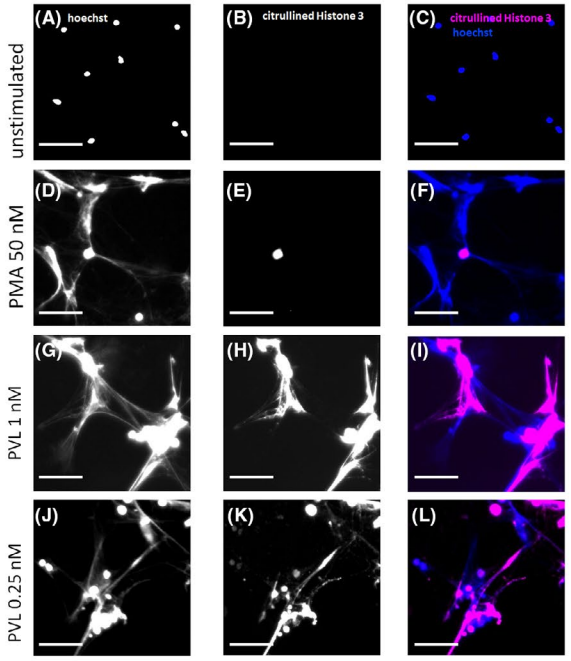

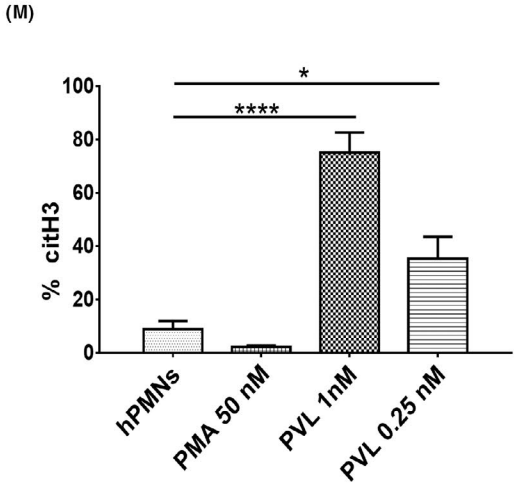

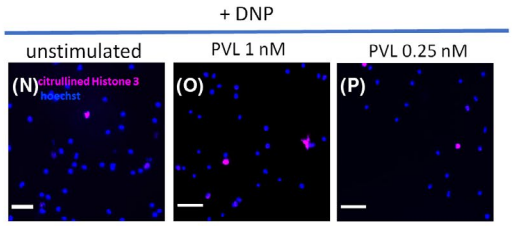

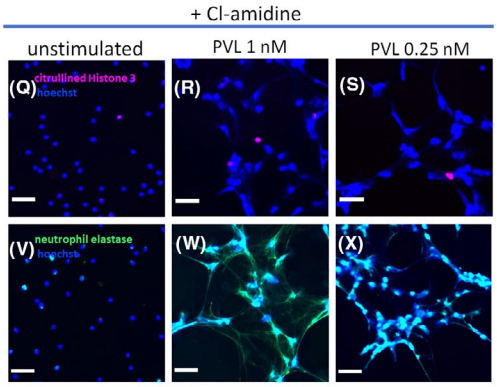

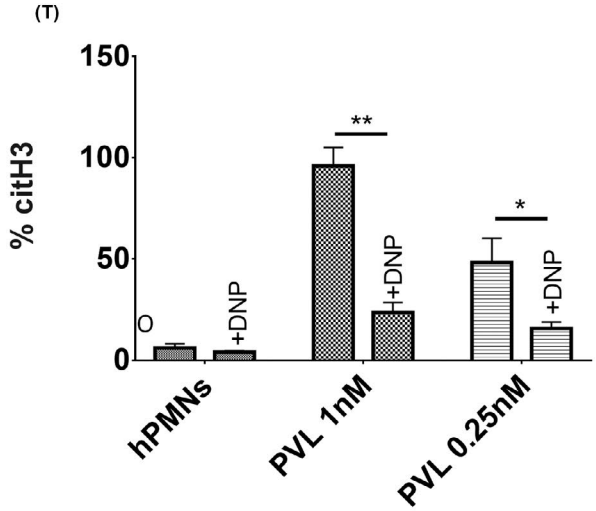

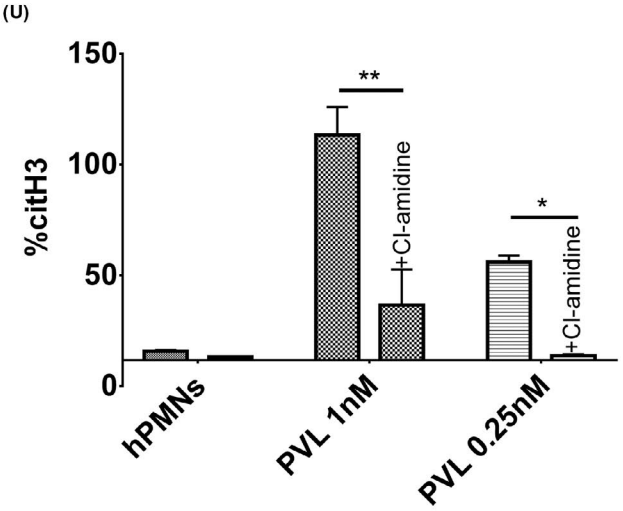

FIGURE 4 PVL, but not PMA, presents citrullinated histone 3 on NETs, depending on PAD4 activity. (A-L) Immunofluorescence staining of anti-citrullinated histone H3 (in pink), DNA, and nuclei are labeled with Hoechst dye (in blue). Human neutrophils (hPMNs) were left unstimulated (A-C) or exposed to 50 nM of PMA (D-F), PVL at 1 nM (G-I) or 0.25 nM (J-L) after 6 hours. Scale bar = 50 μm. M, citH3-positive cells were quantified using eight fields of view obtained from six different biological replicates. Presented is the mean with SEM. Groups were compared using repeated measures one-way ANOVA, $****P \leq .0001$, $*P < .05$. N = 6. (N-S) Immunofluorescence staining of anti-citrullinated histone H3 (in pink), DNA, and nuclei are marked with the Hoechst dye (in blue) in the presence of DNP or Cl-amidine. Human neutrophils (hPMNs) left unstimulated (N and Q) or exposed to PVL at 1 nM (O and R), 0.25 nM (P and S) after 6 hours in the presence of 750 μM of DNP (N-P) or 200 μM of Cl-amidine (Q-S) are stained for citH3 (in pink) and DNA (in blue). (V-X) hPMNs pretreated with 200 μM of Cl-amidine (Q-S) are stained for NE (in green) and DNA (in blue). Scale bar = 50 μm. T, citH3-positive cells were quantified using eight fields of view obtained from three different biological replicates with and without DNP. Presented is the mean with SEM. Groups were compared using repeated measures one-way ANOVA, $**P \leq .01$, $*P < .05$. N = 3. (U) citH3-positive cells were quantified using eight fields of view obtained from three different biological replicates with and without Cl-amidine. Presented is the mean with SEM. Groups were compared using repeated measures one-way ANOVA, $**P \leq .01$, $*P < .05$

pathway. A selective Src inhibitor, the PP2 was used alone or in combination with another Src inhibitor, PP1. These inhibitors are used to consider the effect of Src on PVL- and PMA-induced NETs, by blocking different members of the Src family.[49-52] Surprisingly, our immunofluorescent assays show that PMA NETosis seems partially inhibited by the pretreatment with the combination of the Src family kinase inhibitors PP1 and PP2 (Figure 5I) and by PP2 alone (Figure 5J), showing NETs in only about 30% of hPMNs (Figure 5Q). Conversely, PVL NETosis is not significantly inhibited by PP1 and PP2. (Figure 5L,M,O,P) as NETs are still present in more than 50% of hPMNs (Figure 5Q).

To confirm the previous result, we studied the Src phosphorylation by immunoblots at three different time-points using a specific antibody targeting phospho-Tyr416, the main phosphorylation site that leads to the activation of Src kinases. Our results do not show a significant difference in Tyr416 phosphorylation in contact with PMA or PVL at any time-point we tested, even though a slight disparity in Src phosphorylation can be detected in immunoblot bands at 10 minutes (Figure 5R,S). Thus, PVL does not activate the Akt-ERK pathway, unlike PMA. Additionally, the intracellular signaling pathway downstream the CD45 stimulation, which is operated by the LukF-PV subunit, is unrelated to Src kinase family phosphorylation.

3.6 | Increased and parallel autophagy process occurs during PVL NETosis

Remijsen et al[27] described the induction of autophagy at early times and the requirement of this process during NETosis. Therefore, we investigated the ratio between the light chain of microtubule-associated protein 1A and 1B (LC3A and LC3B). In fact, during autophagosome formation, the lipidation of LC3A leads to LC3B production, which localizes in the double membrane of autophagosomes. Thus, the LC3B/LC3A ratio constitutes an appropriate marker to evaluate the autophagic process. We proceeded with different immunoblot assays to assess and quantify the LC3B/LC3A ratio which increases during autophagy. hPMNs were thus exposed to PMA at 50 nM, PVL at 1 nM and 0.25 nM or left unstimulated during 10, 15, 30, and 100 minutes. Our results indicate that both 1 nM of PVL and 50 nM of PMA trigger a significant increase of LC3B/LC3A ratio after 30 minutes (Figure 6C,D), which represents about 3 folds of the ratio of unstimulated cells (Figure 6E). However, 0.25 nM of PVL failed to significantly increase the LC3B/LC3A ratio, not reaching a statistically appreciable amount of autophagy, but still showing almost twice of the LC3B/LC3A ratio compared to unstimulated cells (Figure 6C–E).

To assess the importance of autophagy for the general mechanism of PVL NETosis, we pretreated hPMNs with either an early-phase or late-stage inhibitors of the autophagy pathway, Wortmannin (Figure 6F–M) and Bafilomycin A1 (Figure 6O–V), respectively, prior to cells stimulation. Our results show that, unlike PMA, PVL-induced autophagy is not necessary for NETosis, as the leukotoxin still triggers NETs release from hPMNs in presence of those inhibitors (Figure 6N,W). Thus, autophagy is involved in both PMA and PVL NETosis, but it represents a parallel and probably independent process during the leukotoxin-induced mechanism.

3.7 | Part of PVL colocalizes with mitochondria after 30 minutes of exposure

Genestier et al and Zimmermann-Meisse et al found that PVL internalizes into hPMNs and subsequently colocalizes with neutrophil subcellular compartments.[21,53] Since mitochondria appear to be "the hubs" of cellular signaling involved in the PVL NETosis, we wondered whether PVL tends to physically interact with this organelle. To answer this additional question, we performed separate confocal microscopy experiments using two specific antibodies to estimate the colocalization of PVL S subunit and the cytochrome C (CytC), a hemoprotein involved in the electron transport at the intermembrane space of the mitochondrion. hPMNs

exposed to the LukS-PV subunit without the corresponding LukF-PV subunit were used as a control, because the absence of the F subunit prevents the entry of PVL into target cells, and thus, the activity of the leukotoxin.[13,15,21] Indeed, we observed that the fluorescence of labeled LukS-PV subunits applied alone is mostly found outside of the plasma membrane of hPMNs (Figure 7A–L). In contrast, after 30 minutes of incubation with 1 nM of PVL, the LukS-PV and CytC signals partially overlap (Figure 7M–X, white arrows). Moreover, the Pearson Correlation Coefficient (PCC) of segmented images results significantly increased compared to the PCC of control hPMNs exposed to LukS-PV subunit alone, showing a P value < .0001 (Figure 7A1,C1,E1). This result has been confirmed by the analysis of the area of the S subunit fluorescence overlapping with the cytochrome C fluorescence area: after 30 minutes from PVL addition, this overlap is found significantly increased compared to hPMNs exposed to S subunit alone, with a P value < .0001 (Figure 7B1,D1,F1). Moreover, we quantified the colocalization between LukS-PV and a fluorescent dye that stains mitochondria, MitoTracker Deep Red FM. Our previous results are further confirmed by this additional analysis (Figure S3). This suggests a possible

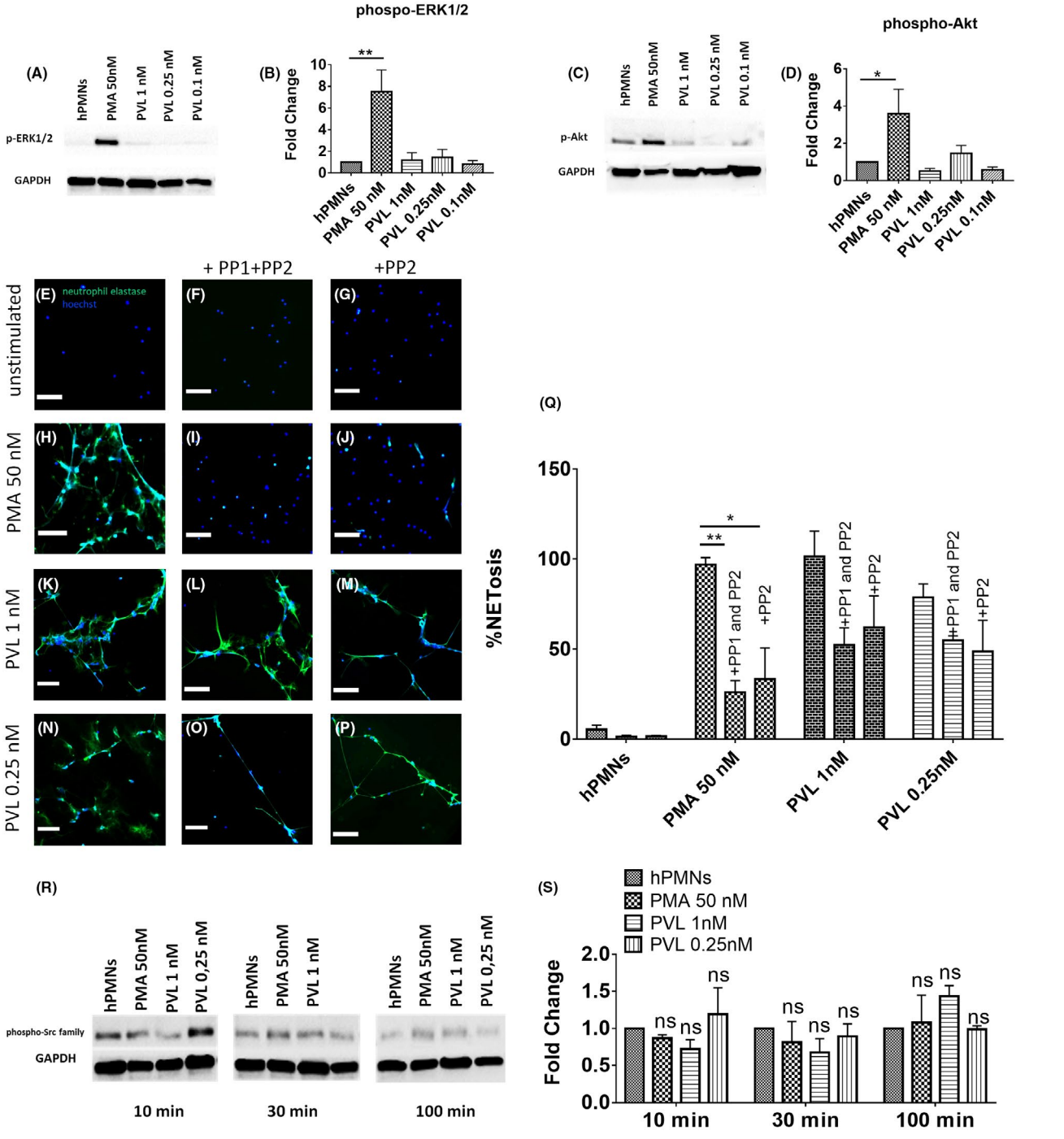

FIGURE 5 ERK1/2 and Akt kinases are not phosphorylated by PVL, while CD45 downstream kinases are not involved in PVL NETosis. (A) Freshly isolated hPMNs are stimulated 50 nM of PMA, 1 nM, 0.25 nM, and 0.1 nM of PVL or in absence of stimuli for 15 minutes, lysed, and probed to detect ERK1/2 phosphorylation by immunoblotting. GAPDH in whole lysates is shown as a loading control. (B) Quantification of ERK1/2 phosphorylation based on fold-change differences of optical density using Image J software. Bands are normalized with correspondent negative control (hPMNs) and GAPDH. Statistical analysis is performed with one-way ANOVA, $^{**}P \leq .01$. Analyzed data of four separate biological replicates. (C) Freshly isolated hPMNs are stimulated 50 nM of PMA, 1 nM, 0.25 nM, and 0.1 nM of PVL or in absence of stimuli for 15 minutes, lysed, and probed to detect Akt phosphorylation by immunoblotting. GAPDH in whole lysates is shown as a loading control. (D) Quantification of Akt phosphorylation based on fold-change differences of optical density using Image J software. Bands are normalized with correspondent negative control (hPMNs) and GAPDH. Statistical analysis is performed with one-way ANOVA, $^{*}P < .05$. Analyzed data of three separate biological replicates. (E-P) Immunofluorescence staining Neutrophil Elastase (in green) and DNA and nuclei (in blue) in the presence or absence of PP1 and PP2. Human neutrophils (hPMNs) were left unstimulated (E-G) or exposed to PMA at 50 nM (H-J) PVL at 1 nM (K-M) and 0.25 nM (N-P), after 6 hours in the absence or presence of the combination of Src inhibitors PP1 at 5 μM and PP2 at 10 μM (F, I, L, and O) or only pretreated 30 minutes with 10 μM of PP2 (G, J, M, and P). Scale bar = 50 μm. (Q) NE-positive cells were quantified using eight fields of view obtained from three different biological replicates with and without Src inhibitors. Presented is the mean with SEM. Groups were compared using repeated measures one-way ANOVA, $^{**}P \leq .01$, $^{*}P < .05$. R, Phosphorylation of Src kinases family residue Tyr416 in hPMNs exposed to 50 nM of PMA, 1 nM or 0.25 nM of PVL or in absence of stimuli at 10, 30, and 100 minutes, detected by immunoblotting. GAPDH in whole lysates is shown as a loading control. (S) Quantification of Src kinases family phosphorylation based on fold-change differences of optical density using Image J software. Bands are normalized with correspondent negative control (hPMNs) and GAPDH. Statistical analysis is performed with one-way ANOVA, ns = nonsignificant. Analyzed data of three separate biological replicates

physical interaction between PVL and mitochondria that produce a significant amount of mtROS after 30 minutes (Figure 2U), reinforcing the idea that this time-point is important for the kinetic and outcomes of PVL on hPMNs in vitro. Moreover, this result is consistent with the previously published work of Genestier and colleagues.[53]

4 | DISCUSSION

Pathogenic bacteria and human immune response evolve as parallel and dynamic processes. This is particularly evident for a widespread bacterium as *Staphylococcus aureus*. Thus, it is not surprising that staphylococcal infections are still a major health challenge in many countries, as this pathogen adapts to hosts and overpasses innate immunity through the contribution of a large panel of virulence factors and toxins, such as PVL. Indeed, *Staphylococcus aureus* reveals an unexpectedly complex strategy to bypass the first line of the human defense, possibly taking advantage of dead neutrophils. The importance of a deeper understanding of PVL mode of action is needed, owing to the poor prognosis of *S. aureus* PVL^{+}-infected patients and the necessity to find new therapeutic targets.

Here, we detail the mechanism of PVL NETosis in vitro triggered by nanomolar and lower concentrations of the toxin. We can assert that in the presence of a physiological concentration of extracellular Ca^{2+}, this leukotoxin elicits a specific form of human neutrophil cell death after several hours: NETosis. In contrast, HlgCB fails to elicit a significant NETosis (Figure 1P-X). This second staphylococcal bicomponent leukotoxin shares the same S subunit target receptor as LukS-PV, although at a different binding site,[54] and acts differently compared with PVL. Indeed, our result confirms that different outcomes are elicited by these two leukotoxins, as already suggested by previous studies.[15,21] Nonetheless, our data challenge some previous reports,[24,25] as PVL alone represents a sufficient stimulus to mediate an abundant lytic NETosis, as highlighted by the extracellular presence of specific markers associated with DNA, such as NE and MPO.

Also, the combination of PVL and another *S. aureus* leukotoxin, such as HlgCB, may have an impact on NETosis, as the simultaneous expression of PVL and other leukotoxins arise and now represents ~5% of clinical strains.

PVL NETs are generated in a NADPH-independent manner, and the process seems to be slightly increased by NADPH oxidase inhibition (Figure 2Q). This unexpected increased level of NETosis might be linked to the different actions of Protein kinase C (PKC) isoforms α and ζ, which are inversely activated in NOX-dependent and NOX-independent processes,[55] thus, confirming the fundamentally different nature of NETosis inducers.

Moreover, an alternative ROS source is involved in PVL NETosis. In fact, PVL causes a massive generation of mtROS, which is necessary for the PVL NETosis process. This result agrees with previous data describing NADPH oxidase-independent NETosis elicited by calcium ionophores.[37] Nevertheless, despite mitochondrial uncouplers pretreatment of hPMNs significantly decrease PVL NETs, those inhibitors failed to completely abolish the process. Another ROS source, MPO, is necessary to PVL NETosis, as it transforms oxygen peroxide into hypochlorous acid, downstream superoxide generation. Besides, by using Allopurinol, we show that PVL NETosis is almost completely abolished. This encouraging data seems to indicate either a protective role of Allopurinol for mitochondrial membrane integrity and function,[56,57] or the involvement of a different kind of ROS source expressed into hPMNs, Xanthine Oxidase (XO). This enzyme

can enhance mtROS generation through the production of superoxide ions.[36,58-60] Moreover, the effect of PVL on hPMNs mitochondria was previously suggested, as mitochondrial membranes depolarize in the presence of the leukotoxin.[21] Thus, this evidence collectively confirmed the involvement of mitochondria, either directly or through the action of XO. However, XO involvement should be confirmed by further studies.

The involvement of a family of small conductance calcium-activated potassium channels (SK type) is required for both PVL-induced NETs and full mitochondrial oxidative burst, validating, and expanding Douda et al studies.[37]

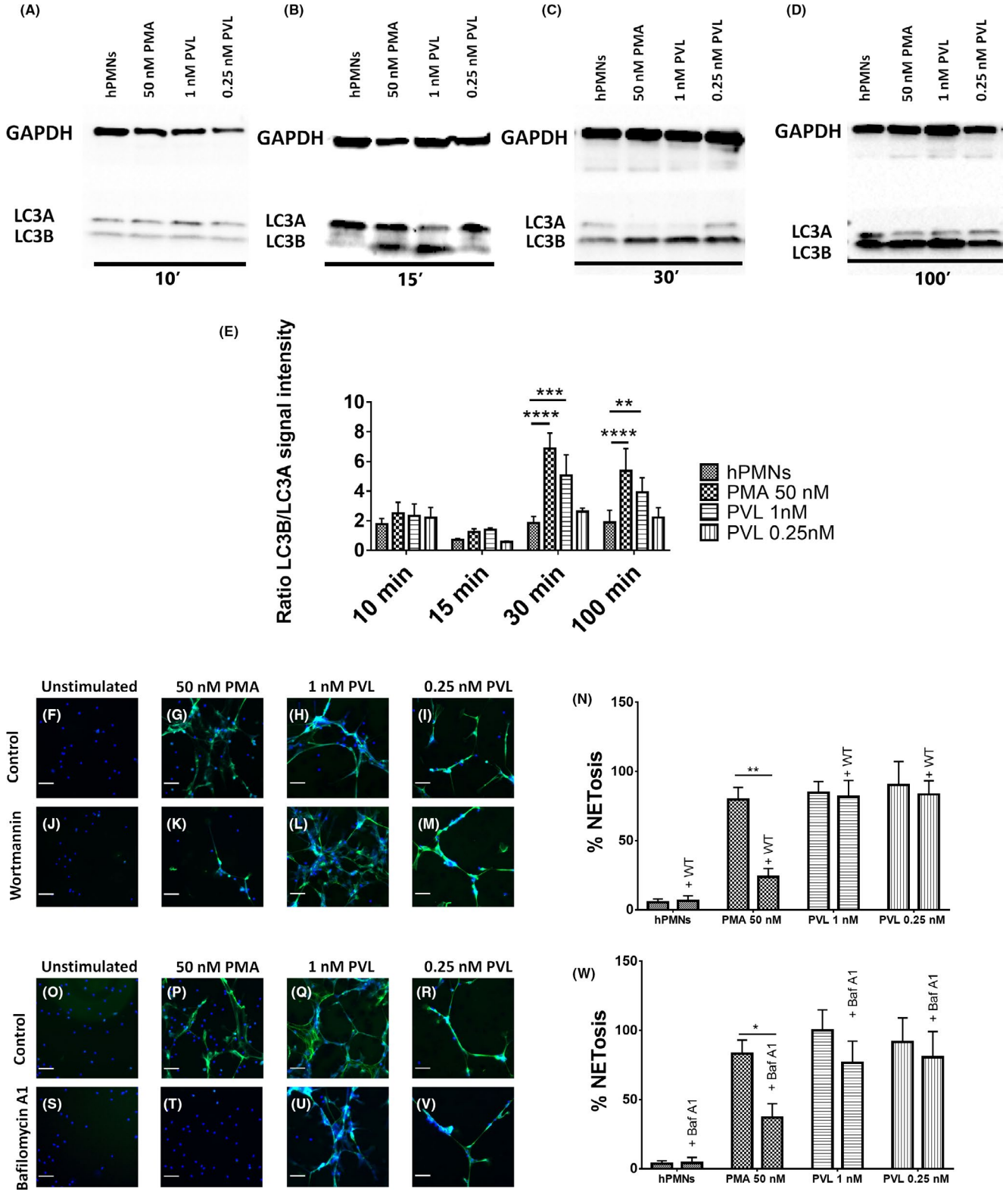

FIGURE 6 Increased and parallel autophagy process occurs during PVL NETosis. (A-D) LC3A and LC3B in hPMNs in the presence of 50 nM of PMA, 1 nM and 0.25 nM of PVL or in the absence of stimuli at 10 minutes (A), 15 minutes (B), 30 minutes (C), and 100 minutes (D), detected by immunoblotting. GAPDH in whole lysates is shown as a loading control. (E) Quantification of LC3B/LC3A ratio based on optical density using Image J software. Bands are normalized with corresponding negative control (hPMNs). Statistical analysis is performed with one-way ANOVA, $****P \leq .0001$, $***P \leq .001$, $**P \leq .01$. Representative images of three or more biological replicates. (F-M) Immunofluorescence images of hPMNs left untreated or stimulated with PMA at 50 nM, PVL at 1 nM or 0.25 nM, during 6 hours, in the presence or absence of 100 nM of Wortmannin and labeled with Hoechst and anti-NE antibody. Scale bar = 50 μm. (N) NE-positive cells were quantified using eight fields of view obtained from four different biological replicates. Presented is the mean with SEM. Groups were compared using repeated measures two-way ANOVA, and Sidak's multiple comparisons test $**P \leq .01$. (O-V), Immunofluorescence images of hPMNs left untreated or stimulated with PMA at 50 nM, PVL at 1 nM or 0.25 nM, during 6 hours, in the presence or absence of 30 nM of Bafilomycin A1 and labeled with Hoechst and anti-NE antibody. Scale bar = 50 μm. (W) NE-positive cells were quantified using eight fields of view obtained from three different biological replicates. Presented is the mean with SEM. Groups were compared using repeated measures two-way ANOVA, and Sidak's multiple comparisons test $*P < .05$

Indeed, SK activation during PVL NETosis is likely due to the increase of intracellular calcium levels. On the contrary, PMA NETosis is independent of SK channels, as previously demonstrated.[37] Nonetheless, MPO appears to be nonessential for the PMA-triggered NETosis (Figure 3). Albeit the latter result seems to disagree with other authors who demonstrated the importance of MPO for PMA NETosis,[22,31,59,61] data previously obtained by Parker et al showed that a residual activity of about 3% of normal MPO was sufficient to allow PMA-induced NETosis in the presence of one pharmacological inhibitor.[60] In fact, these same authors used a combination of two different MPO inhibitors to completely impede MPO activity.[60] Moreover, Kenny and collaborators stated that PMA NETosis was significantly decreased in the presence of 300 μM of the same MPO inhibitor we used for our tests, which is threefolds the concentration we applied to treat hPMNs.[22]

Concerning the intracellular signaling pathway, we showed that the PVL-induced NETosis differs on kinase contribution, compared to the NOX-dependent process (Figure 5), which was previously described for ionophores-induced NETosis.[29,37,62,63] Unexpectedly, the downstream pathway activated by CD45, the main and specific receptor of PVL F subunit,[18] does not seem necessary, nor involved in the PVL process. This suggests a distinct intracellular activation and questions about CD45 contribution during the infection. Conversely, PMA NETosis seems to be partially blocked by Src inhibitors, while no appreciable phosphorylation of Src kinases has been directly observed. This data might be explained by the effect of PP2, the selective inhibitor of Src kinases we used in our experiments. In fact, this compound was previously associated with a decrease of ERK and p38 phosphorylation, which are two main kinases involved in PMA NETosis.[37]

We checked the presence of deiminated histone H3 on NETs, as different reports outlined contradictory data.[37,55,64] In fact, during NETs spread, all cytoplasmic and nuclear content are ejected in the form of an extracellular chromatin network decorated with antimicrobial proteins and peptides. Hence, histones are an integral part of NETs. Therefore, it is not surprising to find H3-positive cells when NETosis is established, rather explained by the fact that histones possess an intrinsic antimicrobial function.[65-68] Nevertheless, this antimicrobial activity could be diminished or inhibited by Arginine residues citrullination. Hence, the detection of citH3 on PVL-induced NETs, but not on PMA-induced NETs (Figure 4), is consistent with previous data reporting that "classical" antimicrobial NOX-dependent NETosis does not involve citrullination.[38] In fact, the NOX-dependent NETosis requires PKCα phosphorylation, which in turn, has been related to peptidyl adenosine deiminase 4 (PAD4) inhibition, impeding citrullination.[55]

Also, PVL-induced citrullination of the histone H3 is confirmed to be directly caused by PAD4, which is a neutrophil calcium-dependent enzyme. This aspect could likely relate to the rapid increase of intracellular calcium triggered by this leukotoxin in hPMNs.[15] Nevertheless, the PADs inhibition performed through Cl-amidine pretreatment does not elicit PVL NETosis (Figure 4), suggesting that H3 citrullination occurs after or independently of NETs extrusion. This result is in contrast with the hypothesized role of PADs as inducers of heterochromatin decondensation and chromatin unfolding through the loss of positive charge of histones during NETosis. Indeed, our data highlight a peculiar aspect, which is exclusively found during PVL NETosis. In contrast, DNP decreases extracellular citH3. This aspect might relate to the inhibition of the main ROS source necessary to the PVL NETosis, which probably blocks the process at its early stage, preventing histone H3 citrullination.

On the contrary, the presence of citrullinated proteins during NETosis has been acutely analyzed by Koenig et al,[38] pointing out that, in general, NETosis can be confused with other forms of DNA extrusion that have morphologically similar consequences on hPMNs, despite being *de facto* biologically different processes. Moreover, Koenig and Andrade[38] demonstrated that the citrullination of a great variety of proteins, named hypercitrullination, provoked with 30 nM and 100 nM of PVL. This particular outcome could ensure a decrease in the antimicrobial activity of the chromatin network, by disabling the arginine

residues, which are critical for antimicrobial action of proteins like histones, elastase, or myeloperoxidase.[68-71] Therefore, *S. aureus* might gain an advantage from this particular form of NETosis, because strains always produce a potent DNAse, and catalase and a superoxide dismutase, thus, allowing the digestion of NETs while creating a local aerobic condition after getting rid of the ROS produced during NETosis. Also, high oxygen concentrations positively regulate PVL expression.[12] Thus, *SA*-expressing PVL could easily overpass and may provide disruption of neutrophil immunity, as well as providing essential nutriments for the bacterium, represented by neutrophil debris.

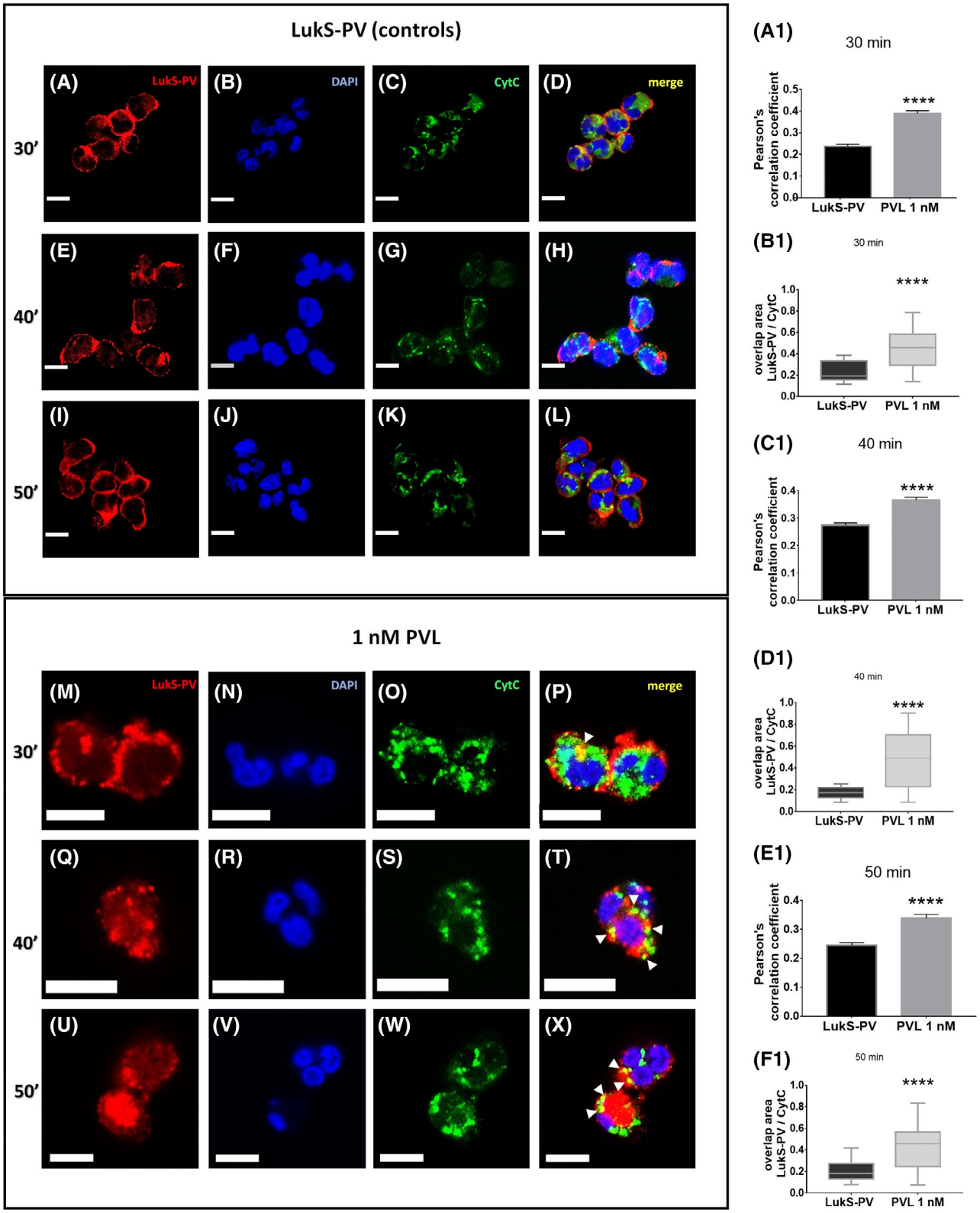

FIGURE 7 Part of PVL colocalizes with mitochondria after 30 minutes of exposure. Freshly isolated hPMNs are exposed from 5 to 50 minutes to either LukS-PV subunit only at 1 nM, used as a negative control (A-L), or to 1 nM of PVL (M-X), presenting both S and F subunits. Figures show representative confocal images of LukS-PV controls at 30 minutes (A-D), 40 minutes (E-H), and 50 minutes (D-L) after S subunit addition (upper box), while 1 nM of PVL was applied for 30 minutes (M-P), 40 minutes (Q-T), or 50 minutes (U-X) in underneath images (lower box). hPMNs were maintained at 37°C with 5% of CO_2 for 5, 10, 15, 20, 30, 40, and 50 minutes. This last time-point was chosen as the cells began to lose their internal organization after 1 hour of exposition to the PVL at 1 nM. After each time-point cells were fixed with 4% of PFA and permeabilized with 0.05% of Triton X-100. Then, two antibodies were applied, anti-CytC antibody (in green) and anti-LukS-PV antibody (in red), to immunolabel mitochondria and the LukS-PV, respectively. DAPI was used to stain nuclei and DNA (in blue). The merged images show the colocalization point between PVL and mitochondria (in yellow), which are additionally highlighted with white arrows. (A1, C1 and E1) Pearson's correlation coefficient (PCC) was quantified using Fiji by Image J plugin Squassh by analyzing about 10 fields of view obtained from three different biological replicates at 30 minutes (A1), 40 minutes (C1), and 50 minutes (E1), which represent the significantly different time-points in terms of PCC between PVL and LukS-PV. Presented is the mean of pooled data with SEM. Groups were compared using Student's *t* test, $^{****}P \leq .0001$. (B1, D1, and F1). The overlapping area of LukS-PV and CytC fluorescence was quantified by using Image J analysis of the same 10 fields of view as for PCC assessment. Shown are the means of pooled data with SEM after 30 minutes (B1), 40 minutes (D1), and 50 minutes (F1), which represent the three significantly different time-points in terms of overlapping area between PVL and LukS-PV alone

Concerning autophagy, this process was previously associated to NETosis[24] and found to be increased, but not necessary for PVL-induced NETosis. This observation might relate to mitochondrial ROS release, which could induce a parallel autophagic process at early times. In fact, superoxide radical is the main form of ROS known to stimulate autophagy,[72] while mitochondria, probably damaged by PVL, could induce an autophagic process known as mitophagy in response to depolarization. Therefore, hPMNs exposed to PVL might present increased autophagy in the attempt to get rid of defective organelles.

Finally, the mitochondrial stress prompted by PVL (Figure 2U) is associated with a partial colocalization between the leukotoxin and mitochondria in hPMNs (Figure 7). This result, albeit not definitive, might complete the mechanism of intracellular trafficking described by Zimmermann-Meisse et al, while confirming the PVL-mitochondria interaction described by Genestier et al.[53] Besides, our images show that hPMNs nuclei exposed to 1 nM of PVL rapidly decondensed, occupying almost the whole cellular space and pushing all cytoplasmic elements toward the plasma membrane. This last aspect must be taken into account as the assumed location of PVL might rather be due to the decrease in available cytoplasm, than to a direct effect of PVL on mitochondria. Nevertheless, the toxin remains located neither in the cytoplasm nor inside the nucleus,[21,53] while likely associates to intracellular membranes. The specific physical interaction between PVL and the nuclear membrane, and/or mitochondrial membrane, remains to be assessed to confirm previous electron microscopy results.[53]

Very little is known about HlgCB consequences on human neutrophils, albeit the toxin is present in 99% of *S. aureus* strains. In fact, HlgCB does not elicit apoptosis, NETosis or membrane permeabilization in human neutrophils per se. Further studies will aim to complete this complex signaling process to evaluate the efficacity of NETosis blockers in infectious models.

In conclusion, while confirming that no pore is produced at the plasma membrane in physiological Ca^{2+} conditions, the action of Panton-Valentine Leukocidin contributes to the severity of human infections. In fact, we can reasonably assume that in the presence of extracellular Ca^{2+} a more complicated process is operated by PVL, a form of NOX-independent NETosis. This phenomenon starts with each leukotoxin subunit binding to its specific membrane receptor, which in turn leads to the endocytosis of the PVL into hPMNs. In parallel, cytosolic intracellular Ca^{2+} is rapidly mobilized from Endoplasmic Reticulum at early times,[15] and a strong mitochondrial oxidative response is described after 30 minutes. The latter might hypothetically occur through a direct interaction between PVL and mitochondrial membranes. Parallelly, the mitochondrial involvement could be sustained by the contribution of another superoxide source, such as the xanthine oxidase, albeit this data needs further confirmations. The increase of intracellular Ca^{2+} triggers the activation of the SK channels and PADs, which induces protein deimination or citrullination. Therefore, during infection, this mechanism may participate in the evasion and dissemination of *SA*, somehow disrupting and producing an upheaval in the human innate immune system.

ACKNOWLEDGMENTS

The authors are particularly grateful to Daniel Keller for the constant support, the recollection of unpublished results in frequent scientific discussions, and the skillful preparation of leukotoxins. Viola Mazzoleni was awarded a doctoral grant from the Ministère de l'Enseignement Supérieur et de la Recherche to perform her doctoral studies. The experimental work was supported by grants from Direction de la Recherche (University of Strasbourg), by funds provided by industrial activity (CONECTUS) of UR-7290, the LabEx (Laboratory of Excellence) MitoCross (National Program PIA), and The Graduate School IMCBio (PIA3 - ANR). The authors thank the Institut de Biologie

Moléculaire des Plantes (IBMP) of Strasbourg for confocal imaging facilities and the Etablissement Français du Sang (EFS) of Strasbourg for providing human buffy coats. This manuscript was proofread by SpringerEdit Proofreading Inc. (Toronto, Canada).

CONFLICT OF INTEREST

The funding agencies had no role in any of the study design, data collection and analysis, decision to publish, or preparation of the manuscript. None of the results obtained are part of a patent or commercial product. G.P. is a permanent faculty member of the University of Strasbourg, IT is a permanent researcher in the CNRS and affiliated to the University of Strasbourg, AS is supported by the LabEx MitoCross. None of the authors has a conflict of interest to declare.

AUTHORS CONTRIBUTIONS

V. Mazzoleni and G. Prévost conceived and designed the experiments, G. Zimermann-Meisse participated in epifluorescence assays. A. Smirnova and I. Tarassov participated in the conception, implementation, and funding of confocal microscopy assays. V. Mazzoleni performed the experiments and prepared the figures. V. Mazzoleni and A. Smirnova analyzed confocal microscopy data. G. Zimmermann-Meisse conceived the sequence of modules for NETosis quantification performed with CellProfiler. V. Mazzoleni wrote the manuscript. V. Mazzoleni, A. Smirnova, I. Tarassov, and G. Prévost revised the manuscript.

ORCID

Viola Mazzoleni https://orcid.org/0000-0003-2067-3758
Ivan Tarassov https://orcid.org/0000-0001-8763-6703
Gilles Prévost https://orcid.org/0000-0002-0419-7766

REFERENCES

1. VandenBergh MFQ, Yzerman EPF, Van Belkum A, Boelens HAM, Sijmons M, Verbrugh HA. Follow-up of *Staphylococcus aureus* nasal carriage after 8 years: redefining the persistent carrier state. *J Clin Microbiol*. 1999;37:3133-3140.
2. Lowy FD. Medical progress: *Staphylococcus aureus* infections. *N Engl J Med*. 1998;339:520-532.
3. Chessa D, Ganau G, Mazzarello V. An overview of *Staphylococcus epidermidis* and *Staphylococcus aureus* with a focus on developing countries. *J Infect Dev Ctries*. 2015;9:547-550.
4. Tong SYC, Davis JS, Eichenberger E, Holland TL, Fowler VG. *Staphylococcus aureus* infections: Epidemiology, pathophysiology, clinical manifestations, and management. *Clin Microbiol Rev*. 2015;28:603-661.
5. Boyle-Vavra S, Daum RS. Community-acquired methicillin-resistant *Staphylococcus aureus*: the role of Panton-Valentine leukocidin. *Lab Investig*. 2007;87:3-9.
6. Shallcross LJ, Fragaszy E, Johnson AM, Hayward AC. The role of the Panton-Valentine leucocidin toxin in staphylococcal disease: a systematic review and meta-analysis. *Lancet Infect Dis*. 2013;13:43-54.
7. Prévost G, Cribier B, Couppié P, et al. Panton-valentine leucocidin and gamma-hemolysin from *Staphylococcus aureus* ATCC 49775 are encoded by distinct genetic loci and have different biological activities. *Infect Immun*. 1995;63:4121-4129.
8. Supersac G, Prévost G, Piémont Y. Sequencing of leucocidin R from *Staphylococcus aureus* P83 suggests that staphylococcal leucocidins and gamma-hemolysin are members of a single, two-component family of toxins. *Infect Immun*. 1993;61:580-587.
9. Aires-de-Sousa M, Conceição T, De Lencastre H. Unusually high prevalence of nosocomial panton-valentine leukocidin-positive *Staphylococcus aureus* isolates in cape verde islands. *J Clin Microbiol*. 2006;44:3790-3793.
10. Breurec S, Fall C, Pouillot R, et al. Epidemiology of methicillin-susceptible *Staphylococcus aureus* lineages in five major African towns: high prevalence of Panton-Valentine leukocidin genes. *Clin Microbiol Infect*. 2011;17:633-639.
11. Otto M. *Staphylococcus aureus* toxins. *Curr Opin Microbiol*. 2014;17:32-37.
12. Finck-Barbançon V, Prévost G, Piémont Y. Improved purification of leukocidin from *Staphylococcus aureus* and toxin distribution among hospital strains. *Res Microbiol*. 1991;142:75-85.
13. Spaan AN, Henry T, Van Rooijen WJM, et al. The staphylococcal toxin panton-valentine leukocidin targets human C5a receptors. *Cell Host Microbe*. 2013;13:584-594.
14. Meyer F, Girardot R, Piémont Y, Prévost G, Colin DA. Analysis of the specificity of panton-valentine leucocidin and gamma-hemolysin F component binding. *Infect. Immun*. 2009;77:266-273.
15. Tawk MY, Zimmermann-Meisse G, Bossu JL, et al. Internalization of staphylococcal leukotoxins that bind and divert the C5a receptor is required for intracellular Ca^{2+} mobilization by human neutrophils. *Cell Microbiol*. 2015;17:1241-1257.
16. Jover E, Tawk MY, Laventie BJ, Poulain B, Prévost G. Staphylococcal leukotoxins trigger free intracellular Ca^{2+} rise in neurones, signalling through acidic stores and activation of store-operated channels. *Cell Microbiol*. 2013;15:742-758.
17. Liu X, Heitz P, Roux M, et al. Panton-Valentine leukocidin colocalizes with retinal ganglion and amacrine cells and activates glial reactions and microglial apoptosis. *Sci Rep*. 2018;8:2953.
18. Tromp AT, Van Gent M, Abrial P, et al. Human CD45 is an f-component-specific receptor for the staphylococcal toxin Panton-Valentine leukocidin. *Nat Microbiol*. 2018;3:708-717.
19. Menestrina G, Dalla Serra M, Comai M, et al. Ion channels and bacterial infection: the case of β-barrel pore-forming protein toxins of *Staphylococcus aureus*. *FEBS Lett*. 2003;552:54-60.
20. Graves SF, Kobayashi SD, Braughton KR, et al. Sublytic concentrations of *Staphylococcus aureus* Panton-Valentine leukocidin alter human PMN gene expression and enhance bactericidal capacity. *J Leukoc Biol*. 2012;92:361-374.
21. Zimmermann-Meisse G, Prévost G, Jover E. Above and beyond c5a receptor targeting by staphylococcal leucotoxins: Retrograde transport of panton–valentine leucocidin and γ-Hemolysin. *Toxins (Basel)*. 2017;9:41.
22. Kenny EF, Herzig A, Krüger R, et al. Diverse stimuli engage different neutrophil extracellular trap pathways. *eLife*. 2017;6:e24437.
23. Brinkmann V, Reichard U, Goosmann C, et al. Neutrophil extracellular traps kill bacteria. *Science (80-)*. 2004;303:1532-1535.
24. Pilsczek FH, Salina D, Poon KKH, et al. A novel mechanism of rapid nuclear neutrophil extracellular trap formation in response to *Staphylococcus aureus*. *J Immunol*. 2010;185:7413-7425.

25. Bhattacharya M, Berends ETM, Chan R, et al. *Staphylococcus aureus* biofilms release leukocidins to elicit extracellular trap formation and evade neutrophil-mediated killing. *Proc Natl Acad Sci USA*. 2018;115:7416-7421.
26. Fuchs TA, Abed U, Goosmann C, et al. Novel cell death program leads to neutrophil extracellular traps. *J Cell Biol*. 2007;176:231-241.
27. Remijsen Q, Berghe TV, Wirawan E, et al. Neutrophil extracellular trap cell death requires both autophagy and superoxide generation. *Cell Res*. 2011;21:290-304.
28. Kaplan MJ, Radic M. Neutrophil extracellular traps: double-edged swords of innate immunity. *J Immunol*. 2012;189:2689-2695.
29. Douda DN, Yip L, Khan MA, Grasemann H, Palaniyar N. Akt is essential to induce NADPH-dependent NETosis and to switch the neutrophil death to apoptosis. *Blood*. 2014;123:597-600.
30. Khan MA, Farahvash A, Douda DN, et al. JNK activation turns on LPS-and gram-negative bacteria-induced NADPH oxidase-dependent suicidal NETosis. *Sci Rep*. 2017;7:3407.
31. Parker H, Dragunow M, Hampton MB, Kettle AJ, Winterbourn CC. Requirements for NADPH oxidase and myeloperoxidase in neutrophil extracellular trap formation differ depending on the stimulus. *J Leukoc Biol*. 2012;92:841-849.
32. Khan MA, Palaniyar N. Transcriptional firing helps to drive NETosis. *Sci Rep*. 2017;7:1-16.
33. Arai Y, Nishinaka Y, Arai T, et al. Uric acid induces NADPH oxidase-independent neutrophil extracellular trap formation. *Biochem Biophys Res Commun*. 2014;443:556-561.
34. Itoh T, Kanmura Y, Kuriyama H. A23187 increases calcium permeability of store sites more than of surface membranes in the rabbit mesenteric artery. *J Physiol*. 1985;359:467-484.
35. Kirchner T, Mller S, Klinger M, Solbach W, Laskay T, Behnen M. The impact of various reactive oxygen species on the formation of neutrophil extracellular traps. *Mediators Inflamm*. 2012;2012:849136.
36. Vergeade A, Mulder P, Vendeville C, Ventura-Clapier R, Thuillez C, Monteil C. Xanthine oxidase contributes to mitochondrial ROS generation in an experimental model of cocaine-induced diastolic dysfunction. *J Cardiovasc Pharmacol*. 2012;60:538-543.
37. Douda DN, Khan MA, Grasemann H, Palaniyar N. SK3 channel and mitochondrial ROS mediate NADPH oxidase-independent NETosis induced by calcium influx. *Proc Natl Acad Sci*. 2015;112:2817-2822.
38. Konig MF, Andrade F. A critical reappraisal of neutrophil extracellular traps and NETosis mimics based on differential requirements for protein citrullination. *Front Immunol*. 2016;7:461.
39. Finck-Barbançon V, Duportail G, Meunier O, Colin DA. Pore formation by a two-component leukocidin from Staphyloccocus aureus within the membrane of human polymorphonuclear leukocytes. *BBA - Mol Basis Dis*. 1993;1182:275-282.
40. Werner S, Colin DA, Coraiola M, Menestrina G, Monteil H, Prévost G. Retrieving biological activity from LukF-PV mutants combined with different S components implies compatibility between the stem domains of these staphylococcal bicomponent leucotoxins. *Infect Immun*. 2002;70:1310-1318.
41. Gauduchon V, Werner S, Prévost G, Monteil H, Colin DA. Flow cytometric determination of Panton-Valentine leucocidin S component binding. *Infect Immun*. 2001;69:2390-2395.
42. Chang JHJHJ, Golland P, Guertin DADA, et al. Cell Profiler: image analysis software for identifying and quantifying cell phenotypes. *Genome Biol*. 2006;7:R100.
43. Brinkmann V, Goosmann C, Kühn LI, Zychlinsky A. Automatic quantification of in vitro NET formation. *Front Immunol*. 2012;3:413.
44. Rebernick R, Fahmy L, Glover C, et al. DNA area and NETosis Analysis (DANA): a high-throughput method to quantify neutrophil extracellular traps in fluorescent microscope images. *Biol Proced Online*. 2018;20:7.
45. Rizk A, Paul G, Incardona P, et al. Segmentation and quantification of subcellular structures in fluorescence microscopy images using Squassh. *Nat Protoc*. 2014;9:586-596.
46. Schindelin J, Arganda-Carreras I, Frise E, et al. Fiji: an open-source platform for biological-image analysis. *Nat Methods*. 2012;9:676-682.
47. Sollberger G, Choidas A, Burn GL, et al. Gasdermin D plays a vital role in the generation of neutrophil extracellular traps. *Sci Immunol*. 2018;3:eaar6689.
48. Wang Y, Li M, Stadler S, et al. Histone hypercitrullination mediates chromatin decondensation and neutrophil extracellular trap formation. *J Cell Biol*. 2009;184:205-213.
49. Fumagalli L, Zhang H, Baruzzi A, Lowell CA, Berton G. The Src family kinases Hck and Fgr regulate neutrophil responses to N -formyl-methionyl-leucyl-phenylalanine. *J Immunol*. 2007;178:3874-3885.
50. Mócsai A, Jakus Z, Vántus T, Berton G, Lowell CA, Ligeti E. Kinase pathways in chemoattractant-induced degranulation of neutrophils: the role of p38 mitogen-activated protein kinase activated by Src family kinases. *J Immunol*. 2000;164:4321-4331.
51. Nijhuis E, Lammers JWJ, Koenderman L, Coffer PJ. Src kinases regulate PKB activation and modulate cytokine and chemoattractant-controlled neutrophil functioning. *J Leukoc Biol*. 2002;71:115-124.
52. Hanke JH, Gardner JP, Dow RL, et al. Discovery of a novel, potent, and Src family-selective tyrosine kinase inhibitor: study of Lck- and FynT-dependent T cell activation. *J Biol Chem*. 1996;271:695-701.
53. Genestier AL, Michallet MC, Prévost G, et al. *Staphylococcus aureus* Panton-Valentine leukocidin directly targets mitochondria and induces Bax-independent apoptosis of human neutrophils. *J Clin Invest*. 2005;115:3117-3127.
54. Spaan AN, Schiepers A, de Haas CJC, et al. Differential interaction of the Staphylococcal toxins Panton-Valentine leukocidin and γ-hemolysin CB with human C5a receptors. *J Immunol*. 2015;195:1034-1043.
55. Neeli I, Radic M. Opposition between PKC isoforms regulates histone deimination and neutrophil extracellular chromatin release. *Front Immunol*. 2013;4:1-9.
56. Lee WY, Lee SM. Synergistic protective effect of ischemic preconditioning and allopurinol on ischemia/reperfusion injury in rat liver. *Biochem Biophys Res Commun*. 2006;349:1087-1093.
57. Karwinski W, Ulvik R, Farstad M, Svardal A, Berge R, Soreide O. Effect of allopurinol on the concentration of endogenous glutathione in hepatocytes after an hour of normothermic liver ischemia. *Eur J Surgery, Acta Chir*. 1993;159:355-359.
58. Urban CF, Ermert D, Schmid M, et al. Neutrophil extracellular traps contain calprotectin, a cytosolic protein complex involved in host defense against *Candida albicans*. *PLoS Pathog*. 2009;5:e1000639.
59. Palmer LJ, Cooper PR, Ling MR, Wright HJ, Huissoon A, Chapple ILC. Hypochlorous acid regulates neutrophil extracellular trap release in humans. *Clin Exp Immunol*. 2012;167:261-268.

60. Parker H, Winterbourn CC. Reactive oxidants and myeloperoxidase and their involvement in neutrophil extracellular traps. *Front Immunol*. 2012;3:424.
61. Akong-Moore K, Chow OA, von Köckritz-Blickwede M, Nizet V. Influences of chloride and hypochlorite on neutrophil extracellular trap formation. *PLoS One*. 2012;7:e42984.
62. Hakkim A, Fuchs TA, Martinez NE, et al. Activation of the Raf-MEK-ERK pathway is required for neutrophil extracellular trap formation. *Nat Chem Biol*. 2011;7:75-77.
63. Keshari RS, Verma A, Barthwal MK, Dikshit M. Reactive oxygen species-induced activation of ERK and p38 MAPK mediates PMA-induced NETs release from human neutrophils. *J Cell Biochem*. 2013;114:532-540.
64. Rohrbach AS, Slade DJ, Thompson PR, Mowen KA. Activation of PAD4 in NET formation. *Front Immunol*. 2012;3:360.
65. Miller BF, Abrams R, Dorfman A, Klein M. Antibacterial properties of protamine and histone. *Science (80-)*. 1942;96:428-430.
66. Hirsch JG. Bactericidal action of histone. *J Exp Med*. 1958;108:925-944.
67. Tagai C, Morita S, Shiraishi T, Miyaji K, Iwamuro S. Antimicrobial properties of arginine- and lysine-rich histones and involvement of bacterial outer membrane protease T in their differential mode of actions. *Peptides*. 2011;32:2003-2009.
68. Cutrona KJ, Kaufman BA, Figueroa DM, Elmore DE. Role of arginine and lysine in the antimicrobial mechanism of histone-derived antimicrobial peptides. *FEBS Lett*. 2015;589:3915-3920.
69. Koziel J, Bryzek D, Sroka A, et al. Citrullination alters immunomodulatory function of LL-37 essential for prevention of endotoxin-induced sepsis. *J Immunol*. 2014;192:5363-5372.
70. Li P, Li M, Lindberg MR, Kennett MJ, Xiong N, Wang Y. PAD4 is essential for antibacterial innate immunity mediated by neutrophil extracellular traps. *J Exp Med*. 2010;207:1853-1862.
71. Sohn DH, Rhodes C, Onuma K, et al. Local joint inflammation and histone citrullination in a murine model of the transition from preclinical autoimmunity to inflammatory arthritis. *Arthritis Rheumatol*. 2015;67:2877-2887.
72. Chen Y, Azad MB, Gibson SB. Superoxide is the major reactive oxygen species regulating autophagy. *Cell Death Differ*. 2009;16:1040-1052.

SUPPORTING INFORMATION

Additional supporting information may be found online in the Supporting Information section.

How to cite this article: Mazzoleni V, Zimmermann-Meisse G, Smirnova A, Tarassov I, Prévost G. *Staphylococcus aureus* Panton-Valentine Leukocidin triggers an alternative NETosis process targeting mitochondria. *The FASEB Journal*. 2020;00:1–22. https://doi.org/10.1096/fj.201902981R